IN VITRO TOXICITY AND INFLAMMATORY RESPONSE INDUCED BY COPPER NANOPARTICLES IN RAT ALVEOLAR MACROPHAGES

THESIS

Brian M. Clarke, Captain, USAF, BSC

AFIT/GES/ENV/08-M01

DEPARTMENT OF THE AIR FORCE
AIR UNIVERSITY

AIR FORCE INSTITUTE OF TECHNOLOGY

Wright-Patterson Air Force Base, Ohio

APPROVED FOR PUBLIC RELEASE; DISTRIBUTION UNLIMITED

The views expressed in this thesis are those of the author and do not reflect the official policy or position of the United States Air Force, Department of Defense, or the United States Government.

AFIT/GES/ENV/08-M01

IN VITRO TOXICITY AND INFLAMMATORY RESPONSE INDUCED BY COPPER NANOPARTICLES IN RAT ALVEOLAR MACROPHAGES

THESIS

Presented to the Faculty

Department of Systems and Engineering Management

Graduate School of Engineering and Management

Air Force Institute of Technology

Air University

Air Education and Training Command

In Partial Fulfillment of the Requirements for the

Degree of Master of Science in Environmental Engineering and Science

Brian M. Clarke, BS

Captain, USAF, BSC

March 2008

APPROVED FOR PUBLIC RELEASE; DISTRIBUTION UNLIMITED

AFIT/GES/ENV/08-M01

IN VITRO TOXICITY AND INFLAMMATORY RESPONSE INDUCED BY COPPER NANOPARTICLES IN RAT ALVEOLAR MACROPHAGES

Brian M. Clarke, BS

Captain, USAF, BSC

Approved:

//signed//	7 March 2008
Charles A. Bleckmann (Chairman)	Date
//signed//	7 March 2008
David A. Smith, Lt Col, USAF, BSC (Member)	Date
//signed//	7 March 2008
Saber M. Hussain (Member)	Date

AFIT/GES/ENV/08-M01

Abstract

Nanotechnology is a thriving industry and has the potential to benefit society in numerous ways. However, not all environmental and human health concerns of nanomaterials have been addressed. Thus, the purpose of this research was to investigate the toxicity and inflammation potential (using cytokines TNF-α and IL-6 as indicators) of various sized copper nanoparticles (40, 60, and 80 nm) in rat alveolar macrophages. Toxicity measurements were accomplished by means of *in vitro* techniques and toxicity mechanisms were studied by measuring reactive oxygen species (ROS) production. In addition, cytokine measurements used enzyme-linked immunosorbent assay (ELISA) methods. Results show copper nanoparticles as gravely toxic to rat alveolar macrophages; concentrations of only 10 μg/mL produced cell viability of less than 20 percent and membrane leakage increases of approximately 75 percent. However, the copper nanoparticles did not produce a significant degree of ROS (only 2.5 fold increases). Also, the toxicity showed a dose-dependent relationship, but not a significant size dependency between the various sized copper nanoparticles. Finally, minimal induction of cytokines occurred; however, stimulation of rat alveolar macrophages by lipopolysaccharide (LPS) and subsequent exposure to copper nanoparticles produced elevated levels of both cytokines.

Acknowledgments

I would like to express my appreciation to Dr. Charles Bleckmann, for his guidance and support throughout the course of this thesis effort. I would also like to thank Dr. Saber Hussain for his technical expertise in the field of *in vitro* toxicity methods. Also, thank you to all of the Air Force Research Laboratory personnel who assisted me in my research endeavor. Thank you to Dr. Laura Stolle, Ms. Kathy Szczublewski, and Mr. Craig Murdock for all of the technical help with my laboratory adventures. Finally, thank you to my wife and son for the patience and understanding throughout this entire process.

Brian M. Clarke

Table of Contents

Page

Abstract iv
Acknowledgments v
Table of Contents vi
List of Figures x
List of Tables xii
I. Introduction 1
Background 1
Environmental Implications 3
Problem Identification 4
Research Focus 7
Research Questions 7
Assumption and Limitations 8
Methodology Overview 8
II. Literature Review 10
Nanotoxicity 10
In Vivo Studies. 12
In Vitro Studies. 13
Reactive Oxygen Species. 15
Copper 17
Copper Nanoparticles 21
Respiratory System 24
Macrophages. 24

Page

Cytokines 28

Tumor Necrosis Factor-α. 29

Interleukin-6. 30

TNF-α and IL-6 Studies. 30

Cellular Assays 31

MTS Assay. 31

LDH Assay. 32

ROS Assay. 33

Cytokine Assay. 33

III. Methodology 34

Overview 34

Cell Culture 34

Nanoparticle Solutions 35

Experiment Overview 36

Cell Counting. 36

Cell Plating. 36

Nanoparticle Dosing. 37

Cellular Assays 37

MTS Assay. 37

LDH Assay. 38

Time Study. 39

Page

ROS Assay. 40

TNF-α Assay. 42

IL-6 Assay. 44

Dynamic Light Scattering.....46

Statistical Analysis 47

IV. Results and Analysis.....48

MTS Assay 48

Time Study 49

LDH Assay 51

Reactive Oxygen Species 52

Cytokine Analysis 56

TNF-α Analysis. 57

IL-6 Analysis. 60

Dynamic Light Scattering.....63

V. Discussion 64

Research Questions and Conclusions 64

Suggestions for Further Research.....65

Appendix A. MTS Assay Protocol 67

Appendix B. LDH Assay Protocol.....68

Appendix C. Reactive Oxygen Species Protocol.....69

Appendix D. TNF-α ELISA Protocol 70

Appendix E. IL-6 ELISA Protocol 73

Bibliography 76

Page

Vita 86

List of Figures

Page

Figure 1: Nanotechnology Research Funding (Tsuji, *et al*., 2006:43)..... 5

Figure 2: Haber-Weiss Reaction (Brember, 1998:1071S)..... 20

Figure 3. Chemical structure of MTS and the converted product of Formazan, which is a measure of cell viability (CellTiter 96 AQ_{ueous} One Solution Cell Proliferation Assay Technical Bulletin)..... 32

Figure 4. LDH Chemical Reaction (CytoTox-ONE™ Homogenous Membrane Integrity Assay Technical Bulletin)..... 32

Figure 5. MTS/LDH assay procedures 38

Figure 6. Time study procedures 40

Figure 7. ROS procedures..... 41

Figure 8. Combined MTS results (Cu-40, 60 and 80 nanoparticles)..... 49

Figure 9. Cu-80 nanoparticle time study (≤ 8 hours)..... 50

Figure 10. Combined LDH results (Cu-40, 60 and 80 nanoparticles)..... 52

Figure 11. ROS production at 6 and 24 hours after exposure to Cu-40 nanoparticles 54

Figure 12. ROS production at 6 and 24 hours after exposure to Cu-60 nanoparticles 54

Figure 13. ROS production at 6 and 24 hours after exposure to Cu-80 nanoparticles 55

Figure 14. ROS production at 6 and 24 hours after exposure to Positive Control (hydrogen peroxide)..... 55

Figure 15. TNF-α produced after exposure to Cu-80 nanoparticles..... 58

Figure 16. Combined (Cu-40, 60, 80 and LPS) results of TNF-α produced 60

Page

Figure 17. Combined (Cu-40, 60, 80 and LPS) results of IL-6 produced 62

List of Tables

Page

Table 1. DoD Investment in nanotechnology over the past three years (in millions of dollars) (*Defense Nanotechnology Research and Development Programs*, 2007)..... 6

Table 2. DLS results, 0-and 24-hour time points..... 63

IN VITRO TOXICITY AND INFLAMMATORY RESPONSE INDUCED BY COPPER NANOPARTICLES IN RAT ALVEOLAR MACROPHAGES

I. Introduction

Background

Engineered nanomaterials have many potential benefits for society today and nanotechnology use has increased significantly in recent years. In 2000, President Bill Clinton deemed nanotechnology a top national priority and developed the National Nanotechnology Initiative (National Nanotechnology Initiative). Nanotechnologies, and specifically nanomaterials, are defined by the National Nanotechnology Initiative (NNI) as: on a length scale of 1-100 nanometers, able to control on the atomic scale, and, able to create novel devices with unique properties because of its function and size (Thomas and Sayre, 2005:316). Human exposure to nano-sized materials is not entirely unprecedented; natural particles produced by forest fires and volcanoes, and some viral particles, are in the nano-size range (Oberdörster, E., 2004:1058). However, engineered nanomaterials are manufactured in the laboratory; thus naturally occurring and anthropogenic (i.e., automobile and industrial combustion products) ultrafine and nano-sized particles are excluded (Thomas and Sayre, 2005:316).

Different nanomaterials include nanoparticles, nanotubes, nanowires, and fullerene derivatives (Holsapple, *et al*., 2005:12). Nanomaterials are being utilized in more products as advancements continue in nanotechnology. For example, nanomaterials are currently utilized in electronics, fuel cells, and personal-care products to include sunscreen (Oberdörster, G., *et al*., 2005:825). Nanomaterials have also being used in toothpastes, sanitary ware coatings, and even food products (Hoet, *et al*., 2004).

The small size and highly reactive properties of nanomaterials make them ideal to serve as reaction catalysts (Thomas and Sayre, 2005:318). Nanomaterials possess increased surface areas due to small diameters, and the ability to be more reactive than larger counterparts. Increased surface area and particle quantities can lead to many positive effects. Promising benefits from nanoparticle use include disease treatment in various medicines and sensory use in intracellular mechanisms. Nanoparticles, due to small size, are able to penetrate deeper into various tissues and display greater intracellular uptake (Panyam and Labhasetwar, 2003:330). Uses include nanomaterials as a drug delivery agent or as a biomarker in disease diagnosis (Oberdörster, G., et al., 2005:824). Nanoparticles are close in size to many biomolecules; thus nanoparticles serve as markers to track enzymes and receptor ligands (Thomas and Sayre, 2005:319). Non-viral nanoparticulate systems have been tested as a delivery mechanism for therapeutic agents targeting macrophages because of the vital role macrophages play in the immune system, specifically the inflammatory response (Chellat, *et al*., 2005:7260). Other studies have shown the ability for certain nanoparticles to successfully cross the blood-brain barrier. Kreuter describes how an intravenously administered nano-sized

particle was able to cross the blood-brain barrier to treat intracranially transplanted glioblastomas 101/8 in rats (2001:65).

Environmental Implications

Nanomaterials enter the environment through several routes and can subsequently be transported via different environmental mediums to include air, soil, and water (Oberdörster, G., *et al*., 2005:825). The large surface area and reactive properties of nanoparticles may allow increased persistence in the environment, which can be a useful property in remediation efforts (Holsapple, *et al*., 2005:12). Nanomaterials have been tested for use as potential remediation agents to treat environmental contaminants. For example, iron nanoparticles (Fe^0) have been successfully utilized for the remediation of a trichloroethene (TCE) contaminated water source (Liu, Y., *et al*., 2005:1344). Previous remediation efforts have used iron fillings; however, iron nanoparticles' increased surface-to-volume ratio allows increased reactivity and has been more effective in remediation efforts (Liu, Y., *et al*., 2005:1338). However, the effective transport of nanoparticles in the environment has been limited by particle size in the subsurface. Thus, special delivery methods may be needed for efficient nanoparticle transport to aid in remediation efforts (Schrick, *et al*., 2004:2193).

Another subsequent use for nanomaterials is an antibacterial agent for such items to include certain medical devices (Morrison, *et al*., 2006:138). Fullerene water suspensions (FWS) have previously been tested for their antimicrobial properties against *Escherichia coli*. Fullerene powder (C_{60}) has an extremely low solubility in water; however, one study's aim was to mimic a potential environmental spill of C_{60} powder or

C_{60} and solvent mixture. The study showed that a FWS could be prepared for the antimicrobial evaluation of nC_{60}, which is equivalent to C_{60} when in contact with water or other liquids (Lyon, *et al*., 2006:4360). Lyon and others showed antibacterial properties of the FWS against the test organism *Bacillis subtillis* (2006:4362). E. Oberdörster also showed bactericidal activity of C_{60} in an aquatic environment (2004:1061).

Problem Identification

Despite the potential benefits of nanotechnology, the knowledge base of human health and environmental effects in the production and use of nanomaterials is insufficient. Exposure to nanoparticles can occur through consumer product use and disposal and potential spillage during shipping and handling (Chen, Z., *et al*., 2006:109). In general, nanoparticle toxicity is related to the small particle size, the ease with which the particles move and enter into cells, and the increased surface area of nanoparticles (Dowling, 2004:33). As past experience has shown with other novel products, acceptance of nanotechnology use will largely be based on if the public accepts the potential risks in exchange for the established or promising benefits (Tsuji, *et al*., 2006:42). Even though different nanoparticles display similar properties, not all nanoparticles can be treated as equal and must be studied individually (Holsapple, *et al*., 2005:12). In addition, many nanomaterials present unique properties because of the type of surface coating applied on the material (Thomas and Sayre, 2005:318).

The United States Environmental Protection Agency (EPA) is concerned about the unmanaged use of nanomaterials for various applications and the unknown environmental transport processes that the materials may exhibit. The EPA states,

"*Potentially harmful* effects of nanotechnology may exist. These effects might relate to the nature of nanoparticles themselves, the characteristics of the products made from them, or the aspects of the manufacturing process involved" (US EPA Nanotechnology). In addition, there is little research as to the potential ecotoxic effects of nanoparticles to aquatic organisms. However, one difference exists because prokaryotes do not possess the proper mechanisms for bulk transport of nano-sized particles as compared to eukaryotes (Moore, *et al*., 2006:970). Nanomaterials are under constant investigation by various industries. In recent years, the United States government has attempted to coordinate research and regulatory needs in regards to the environmental, human health, and safety risks of nanotechnology. However, most research involving nanotechnology has focused on application and use. Environmental and human health effects have not been a focus, as evidenced by the research funding shown in Figure 1 below. Overall, human and environmental health research accounts for only four percent of the total nanotechnology research funding budget in the United States (Tsuji, *et al*., 2006:42).

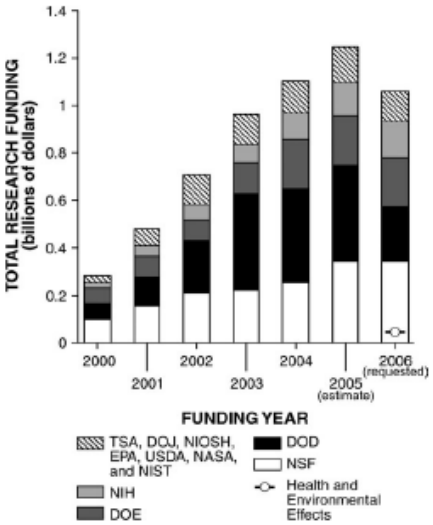

Figure 1: Nanotechnology Research Funding (Tsuji, *et al*., 2006:43)

In addition, the Department of Defense (DoD) has also focused on the benefits of nanotechnology (see Table 1, below). For example, the DoD (through Defense Research and Engineering) produces an annual report, the *Defense Nanotechnology Research and Development Programs*, to discuss DoD nanotechnology programs, current and future research, and recommendations for future activities involving nanotechnology.

Table 1. DoD Investment in nanotechnology over the past three years (in millions of dollars) (*Defense Nanotechnology Research and Development Programs*, 2007)

	FY2006 (Actual)	FY2007 (Estimate)	FY2008 (Request)
Army	64.012	66.984	34.136
Navy	45.460	45.188	27.140
Air Force	89.907	70.855	63.817
DARPA	195.377	219.320	212.458
DDR&E	5.800	5.000	7.200
CBDP	19.882	9.650	39.801
MDA	3.520	0.270	0.130
TOTAL	**423.958**	**417.267**	**374.682**

However, the DoD has also become increasingly concerned with the potential adverse effects of nanoparticles. In July 2004, the United States Air Force funded a five-year, 5.5 million dollar project to develop a model that will ultimately predict biocompatible and toxic effects of nanoparticles (DoD Funds). The Air Force hopes the project will effectively evaluate the physiochemical characteristics of nanomaterials that cause adverse effects, cellular uptake and translocation mechanisms by conducting *in vitro* testing of several nanomaterials that range in sizes from 3 to 100 nm.

Research Focus

Various *in vitro* and *in vivo* studies involving nanoparticles have been conducted; yet little research has been done concerning copper nanoparticle toxicity. One *in vivo* study examined copper nanoparticle toxicity via an ingestion exposure route (Chen, Z., *et al*., 2006). My research focus will be on the use of alveolar macrophages due to the crucial role that alveolar macrophages play within the immune system. Thus, an *in vitro* study of alveolar macrophages is a good model to represent the respiratory system. Different toxicity mechanisms can be measured by *in vitro* studies, and the sensitivity of various nanoparticles can be measured using various cell lines. *In vitro* testing methods provide a rapid and inexpensive method of screening the numerous synthetic chemicals produced every year (Trohalaki, *et al*., 2002:499). However, *in vitro* cytotoxicity tests can be used as a screening method, but not as a replacement for *in vivo* procedures and evaluations.

Research Questions

1.) Are copper nanoparticles (40, 60, and 80 nm) toxic to alveolar macrophages?
2.) Is the toxicity size-dependent (i.e., difference in toxicity between the three sizes of copper nanoparticles)?
3.) Do copper nanoparticles induce reactive oxygen species (ROS)?
4.) Do copper nanoparticles induce an inflammatory response (using cytokines TNF-α and IL-6 as indicators)?

Assumption and Limitations

This research will focus on one cell line (rat alveolar macrophages); thus, not all organ systems can be modeled. In addition, copper nanoparticle transport (i.e., toxicokinetics) throughout the body cannot be described by using an *in vitro* model. For example, if an exposure occurred to a large amount of nanoparticles, the alveolar macrophage clearance mechanisms may become overloaded. The particles, due to the small size, may then be able to cross into epithelial tissue and the interstitial layer. An *in vitro* model will not describe the transport to various organs within the body.

In vitro toxicity testing of nanoparticles present some novel challenges to toxicity testing. Teeguarden and others explain that a nanoparticle dose is not static, but dynamic and can be extremely complicated (2007:300). In addition, other factors, such as particle size, particle number, and diffusion rates of the particle, must be considered during the dosing process (2007:301). One potential problem is the dynamic nature and ability of nanoparticles to "settle, diffuse, and aggregate differentially according to their size, density, and surface physicochemistry," as compared to soluble chemicals (Teeguarden, *et al*., 2007:300-301). In addition, one must account for the dosing solutions used and its applicable properties to include viscosity, density, and protein presence (Teeguarden, *et al*., 2007:301).

Methodology Overview

The methodology used rat alveolar macrophages as the cell line for all *in vitro* toxicity and cytokine experiments. The progression of assays started with basic toxicity experiments (MTS and LDH), followed by mechanism of toxicity (ROS), and finally

inflammation measurements (TNF-α and IL-6). For statistical significance, at least two to three separate experiments were done for each assay with multiple samples of each copper nanoparticle concentration.

II. Literature Review

Nanotoxicity

Nanotoxicology can be defined as the "science of engineered nanodevices and nanostructures that deals with their effects in living organisms" (Oberdörster, G., *et al*., 2005:824). In regards to research on the health effects of nanomaterials, the inhalation exposure route has been extensively studied as compared to the ingestion (via the gastrointestinal tract) or skin absorption routes of exposure (Tsuji, *et al*., 2006:43). More research is needed to determine if nanoparticles can penetrate the skin (Tsuji, *et al*., 2006:44), because little information exists as to whether nanoparticles can be absorbed through the stratum corneum (Holsapple, *et al*., 2005:13). Both *in vivo* and *in vitro* studies have been conducted on the toxicology of airborne nanoparticles found in environmental and occupational settings to include effects on the respiratory system and extrapulmonary organs (Oberdörster, G., *et al*., 2005:825). Many factors contribute to the pulmonary toxicity of nanoparticles to include size, dose to target organ or tissue, surface coating or treatment, degree of aggregates formed, surface charge, and shape (Tsuji, *et al*., 2006:47). However, Vicki L. Colvin explains in "The potential environmental impact of engineered nanomaterials," that, although research has focused on the inhalation exposure route, the more common exposure route may be dermal absorption or oral injection exposure because many nanomaterials are prepared in liquids and agglomerate strongly, making it difficult for them to become respirable nanoparticles (2003:1167). Also, many pulmonary studies have been conducted on ultrafine particles; however, ultrafine particles are not identical to engineered nanoparticles. Ultrafine

particles are less than 100 nm in diameter, but are usually more chemically heterogeneous and polydispersed than engineered nanoparticles (Colvin, 2003:1168).

Nanoparticles also possess the ability to produce systemic effects (Holsapple, *et al*., 2005:15). One potential nanoparticle transport mechanism is via transcytosis directly to the circulation system via the respiratory tract epithelia and interstitium (Hoet, *et al*., 2004; Oberdörster, G., *et al*., 2005:829). Sensory nerve endings in respiratory epithelia may also transport nanoparticles to different central nervous system structures (Oberdörster, G., *et al*., 2005:829). Y. Chen and colleagues show that nanoparticles have the ability to cross the blood-testis barrier (2003:279). Concordingly, Kim and colleagues showed that synthesized biocompatible silica-overcoated magnetic nanoparticles containing rhodamine B isothiocyanate (RITC) within a silica shell of controllable thickness [MNPs@SiO2(RITC)] penetrated the blood-brain barrier and persisted within the body for an extended period of time, but caused no toxicity (2006:346). Nanoparticles also can produce pulmonary inflammatory mediators within the lung that may indirectly affect the circulatory system (Hoet, *et al*., 2004).

Current research has focused on the cellular internalization of nanoparticles. Recent microscopic investigations showed alveolar macrophages internalized nanoparticles, as the particles were surrounded within the cell (Hussain, *et al*., 2005:982). Macrophages isolated from the peritoneal cavity also displayed an active uptake of functionalized carbon nanotubes (Dumortier, *et al*., 2006:1526). Another *in vitro* study showed that nanoparticles were uptaken by J-744 macrophages via endocytosis and ultimately degraded in the lysosomal compartment (Vauthier, *et al*., 2003:526-527).

Furthermore, a different study indicated that a fullerene derivative can cross the cellular membrane towards the mitochondria (Foley, *et al*., 2002:116). However, the exact internalization mechanism is still unknown as it is difficult to determine if particle internalization is due to a cellular or active uptake mechanism.

In Vivo Studies.

A recent *in vivo* experiment showed the development of dose-dependent epitheliod granulomas and interstitial inflammation is mice after intratracheally instilled exposure to single-wall carbon nanotubes during a 7-day and 90-day exposure (Lam, *et al*., 2004:126). In the study, carbon nanotube toxicity was compared against carbon black (CB), a known low-toxicity dust. The study displayed both carbon nanotubes and carbon black uptake by alveolar macrophages; however, the reactions of each material differed once in the lung. Macrophages that phagocytized the CB spread within the alveolar space, while the macrophages containing the carbon nanotubes positioned in centrilobular locations and formed epitheliod granulomas (Lam, *et al*., 2004:131). In addition, the 90-day, carbon nanotube high-dose exposure group displayed more lesions than the 7-day, high-dose group. One reason for this difference was the accumulation of dust within the interstitium, which increased over time and more lesions developed. Also, when dust entered the interstitial or subepithelial space within the lung, it could not be removed by normal macrophage function via the mucociliary escalator system (Lam, *et al*., 2004:131).

In comparison to the Lam, *et al*. study described above, Warheit and colleagues used significantly higher nanoparticle concentrations. Using intratracheally instilled

nanontubes, the study produced results, including mortality, in approximately 15 percent of all rats exposed to high (five mg/kg) doses of single-walled carbon nanotubes (Warheit, *et al*., 2004:117). Also, the toxic effect observed was primarily due to mechanical blocking in the upper airways of the high nanoparticle doses (Warheit, *et al*., 2004:117). In addition, Warheit and colleagues reported a non-dose dependent development of multifocal granulomas (2004:124). Warheit also points out that The National Institute for Occupational Safety and Health (NIOSH) health risk assessments of workplaces manufacturing single-walled carbon nanotubes showed small levels of exposure to respirable-sized carbon nanotubes (not detectable to ≤ 0.1 mg/m^3) (Maynard, *et al*., 2004:106).

Another recent study examined fullerene nanoparticle (nC60) toxicity. Fullerenes possess properties that allow consideration for use as a possible drug delivery system (Oberdörster, E., 2004:1061). In the study, juvenile largemouth bass were exposed to 0.5 parts per million (ppm) of aqueous uncoated fullerenes for 48 hours. The study showed that the fullerenes translocated into the largemouth bass brains via the olfactory bulb (Oberdörster, E., 2004:1058). In addition, the largemouth bass showed lipid peroxidation in the brain tissue and a depletion of glutathione (GSH) within its gills (Oberdörster, E., 2004:1058).

In Vitro Studies.

Recent *in vitro* studies of nanoparticles have demonstrated a wide range of toxic effects. During gameteogenesis, chemicals can have an adverse effect on germlines. One study examined the effects of various nanoparticles on germline stem cells (C18-4).

Silver (Ag-15nm), molybdenum (MoO_3-30nm), and aluminum (Al-30nm) nanoparticles were tested for cytotoxicity effects to include impaired mitochondria function (MTT), lactase dehydrogenase (LDH) leakage, and cellular apoptosis/necrosis (Braydich-Stolle, *et al*., 2005). Molybdenum nanoparticles were the least toxic, displaying toxicity properties only at significantly high dose concentrations ≥ 50 µg/mL. Silver nanoparticles were the most toxic, with a calculated MTT Effective Concetration$_{50}$ (EC_{50}) value of only 8.75 µg/mL and LDH EC_{50} value of 2.50 µg/ml (Braydich-Stolle, *et al*., 2005:418). In comparison, another study using the same silver nanoparticles (Ag-15 nm) showed a significant increase (i.e., reduced toxicity) in the MTT EC_{50} and LDH EC_{50} when using a different cell line (BRL 3A cells) (Hussain, *et al*., 2005:978). In the study, LDH leakage and MTT reduction data also showed that molybdenum (MoO_3-30 nm) nanoparticles were fairly toxic and iron oxide (Fe_3O_4-47nm) and aluminum (Al-30 nm) nanoparticles displayed low toxicity (Hussain *et al*., 2005:982). Wagner and others showed that rat alveolar macrophage exposure to various sized aluminum nanoparticles (50, 80, and 120 nm) showed reduced cell viability after exposures of 100 to 250 µg/mL, while exposure to aluminum oxide nanoparticles (Al_2O_3) showed little toxicity (2007:7358). In addition, the phagocytic ability of the macrophages became impaired at only 25 µg/mL (2007:7359). Finally, as reviewed by Warheit, *et al*., *in vitro* exposure to nano-sized C_{60} fullerenes produced toxicity in both human and bovine alveolar macrophages, to include a 60 percent reduction in cell viability (2004:122).

Reactive Oxygen Species.

Free radicals are species that have one or more unpaired electrons. Reactive oxygen species (ROS) formation is one cause of programmed cell death, or apoptosis (Tan, *et al*., 1998:1423). Oxidative stress can lead to cellular DNA damage to include carcinogenesis initiation and progression and also mutation development (Waris and Ahsan, 2006). Reactive species can cause lung inflammation, lipid peroxidation, and enzyme inactivation (Martin, *et al*., 1997:1302). Numerous oxygen derived species can be formed to include superoxide radical (O_2^-), hydrogen peroxide (H_2O_2), singlet oxygen ($^1O_2$), and hydroxyl radical (·OH) (Waris and Ahsan, 2006). Each reactive species produced has a different biological half-life influencing lethality (Sies, 1997:292).

In normal cellular and transport processes, oxidants are naturally produced as a product of aerobic metabolism (Sies, 1997:291). Also, under normal circumstances, the human lung lies in an equilibrium balance between oxidant and defensive enzymatic and nonenzymatic antioxidant production (Dörger, *et al*., 1997:1311). Many mediators released by alveolar macrophages target specific cell receptors; however, ROS are non-specific and can cause significant tissue damage and injury (Morgan and Shines, 2004:139), especially if produced at higher rates (Sies, 1997:291). In addition, the formation of reactive species leads to the activation of signal transduction pathways and acts as secondary messengers in other cellular pathways (Martin, *et al*., 1997:1301; Forman and Torres, 2001:189).

Nanoparticles can induce ROS formation and have shown a greater inflammatory potential than larger particles (Oberdörster, G., *et al*., 2005:826-827). ROS production

mechanisms include the metabolism of nanoparticles to produce redox active intermediates (Oberdörster, G., *et al*., 2005:828). Another mechanism of ROS production is by the activation and release of NADPH oxidase by alveolar macrophages (Forman and Torres, 2001:189). Attempted phagocytosis can lead to free radical production. An *in vitro* study of vitreous fibers showed that the longer in time the attempted phagocytosis, the greater the amount of ROS created by alveolar macrophages (Dörger, *et al*., 2001a:212).

In the *in vitro* study using BRL 3A cells described above, Ag (15 and 100 nm) nanoparticles produced ROS; thus, the degree of oxidative stress is believed to be one of the primary contributors to nanoparticle cytotoxicity (Hussain, *et al*., 2005:982). Measures of oxidative stress include a depletion of reduced GSH or an increase in oxidized GSH (Hussain and Frazier, 2002:424). GSH is a molecule that plays a role in cellular oxidation-reduction homeostasis (Sies, 1999:916). The depletion of GSH is a good indicator of decreasing antioxidant defenses against reactive oxygen species (Oberdörster, E., 2004:1061). Hussain and colleagues noted that an increase in ROS production correlated with a decrease in GSH, confirming the mechanism of GSH depletion leading to a weakened defense against ROS. Another study showed that an initial ROS increase (5 to 10 fold) is due to a depletion of GSH, while a secondary increase (200 to 400 fold) can be attributed to the mitochondrial electron transport chain (Tan, *et al*., 1998:1423). In the study by Tan and colleagues, a gradual ROS increase was observed during the first six hours, followed by a dramatic increase over the following six hours. The initial, gradual ROS increase lasted until GSH levels fell below 20

percent. After the antioxidant cysteine and GSH depletion, ROS levels increased substantially and at a much faster rate (1998:1429).

Copper

Copper (Cu) is a metal used in numerous applications to include in conductors to distribute electricity and heat. Copper pipes are also used to transport drinking water throughout water distribution systems. Copper normally exists in various states including oxidized cupric (Cu^{2+}), reduced cuprous (Cu^{+}), and metallic copper (0) (Linder and Hazegh-Azam, 1996:797S). In most biological systems, the cupric form is most prevalent (Linder and Hazegh-Azam, 1996:797S). Cupric compounds are blue-green in color and highly soluble in water (Barceloux, 1999:219). In aqueous solutions, cuprous ions commonly dissociate to cupric (II) and metallic copper (Barceloux, 1999:219). Copper is used, as either a metal or an alloy, in machinery, construction, and transportation (Barceloux, 1999:219). Copper is also used in such applications as jewelry, electrical applications, fabrication of dental crowns, dye manufacturing, petroleum refining, metal finishing, and wood preservation (Barceloux, 1999:219). Not only is copper used for production purposes, but the human body utilizes it as well.

Copper is an essential trace element for humans. Normal copper intake levels typically range from 0.6 to 1.6 mg/day with a recommended dietary allowance of 0.9 mg/day (Dietary Reference). However, the contamination of food and water by excess copper can cause severe acute gastrointestinal illnesses (Barceloux, 1999:218). Copper can also be found in drinking water distribution systems, with an established action level of 1.3 mg/L as measured at the 90 percentile limit (US EPA Copper). In surface water

sources, copper concentrations average 10 parts per billion (ppb), while averaging only 5 ppb in groundwater (Dorsey, *et al*., 2004). Copper is found in the atmosphere as a result of natural and anthropogenic sources at a concentration range of 5-200 ng/m^3 (Dorsey, *et al*., 2004). The American Conference of Governmental and Industrial Hygienists (ACGIH) Threshold Limit Value-Time-Weighted Average (TLV-TWA) is 0.2 mg/m^3 for copper fumes and 0.1 mg/m^3 for copper dusts and mists as pertaining to occupational exposures (ACGIH TLV Guide, 2006). Copper is a respiratory irritant to the mouth, eyes, and nose. However, copper metal fumes are rarely produced due to the required high temperatures that are rarely met in normal industrial operations (Barceloux, 1999:225). The International Agency for Research on Cancer or the United States Toxicology Program lists copper as a suspected human or animal carcinogen (Barceloux, 1999:225). Thus, it is important to understand how the human body processes copper.

The human body has natural mechanisms to control cellular uptake, elimination and distribution of copper (Bertinato and L'Abbé, 2004:316). The small intestine serves as the major site of copper absorption and regulation for the human body (Bertinato and L'Abbé, 2004:317). However, the liver serves as the initial site of copper deposition; thus, the liver commonly is the target organ for cytotoxic effects (Gaetke and Chow, 2003:149). Copper is normally attached to proteins in the liver (Seth, *et al*., 2004:501). These proteins, known as copper chaperones, deliver copper to specific targets within a cell (Bertinato and L'Abbé, 2004:316). These same copper chaperones that exist in humans have also been identified in lower eukaryotic organisms (Bertinato and L'Abbé, 2004:316).

A deficiency or excess in copper levels can have detrimental effects on the body. A copper deficiency can lead to Menke's syndrome while a copper overload can cause Wilson's disease (Bertinato and L'Abbé, 2004:317). Menke's syndrome is often fatal during the early childhood years (Gaetke and Chow, 2003:149) and is primarily caused by an inability to transfer copper into the blood from intestinal mucosal cells (Linder and Hazegh-Azam, 1996:799S). Wilson's disease is a genetic disorder that causes ineffective copper metabolism leading to cytotoxic effects and an accumulation of copper in hepatocytes (Seth, *et al*., 2004:501-502). In addition, copper overload can effectively lead to the depletion of GSH and increased cellular toxicity. One mechanism to combat cellular toxicity is by the transfer of excess copper to metallothionein (MT) (Freedman, *et al*., 1989:5603). Metallothioneins normally function to store extra copper and other metal ions and play a role in detoxifying copper (Linder and Hazegh-Azam, 1996:803S).

Even though some levels of copper are required for proper antioxidant defense, copper also leads to the production of reactive oxygen species (Gaetke and Chow, 2003:158). The formation of reactive species is considered the primary mechanism of copper toxicity. Studies show copper can act as a catalyst in ROS production, which can ultimately lead to oxidative stress and lipid peroxidative damage (Stohs and Bagchi, 1995:321). Both forms of copper ions participate in redox reactions, with the amount of ROS produced related to the quantity of free copper ions (Gaetke and Chow, 2003:150). As mentioned previously, copper ions are normally bound to proteins. However, copper ions that become free and accumulate can lead to the formation of reactive hydroxyl radicals (Gaetke and Chow, 2003:147). If reducing agents such as superoxide ($*O_2$),

ascorbic acid, or GSH are present, Cu^{2+} can be reduced to Cu^{+}. The Cu^{+} then can catalyze the reaction of hydrogen peroxide to the formation of hydroxyl radicals (OH^{+}) via the Haber-Weiss Reaction (see Figure 1, below) (Gaetke and Chow, 2003:150). As reviewed by Gaetke and Chow, the hydroxyl radicals are one of the most powerful oxidizing radicals and can react with almost any biological molecule (2003:150) and subsequently affect proteins, lipids, and nucleic acids (Halliwell and Gutteridge, 1984:2).

$$O_2^{\cdot -} + Cu^{2+} \rightarrow O_2 + Cu^{+}$$
$$Cu^{+} + H_2O_2 \rightarrow Cu^{2+} + OH^{-} + OH^{\cdot}$$

Figure 2: Haber-Weiss Reaction (Brember, 1998:1071S)

Other toxicity studies have also demonstrated the effects of copper. Rats exposed via bronchoalveolar lavage (BAL) to equal doses of six different metals showed copper to be the most toxic, as copper was the first metal to produce pulmonary inflammation (Rice, *et al*., 2001:52). The copper exposed rats also had the highest lactate dehydrogenase (indicating membrane leakage and cellular death) and protein levels. In addition, at the low exposure dose, only copper produced neutrophilia in significant levels and at the high exposure dose, copper was the only metal to produce macrophage inflammatory protein (MIP-2) mRNA at the four-hour exposure point, indicating copper to be the most pro-inflammatory metal studied (Rice, *et al*., 2001:46 and 50). An *in vitro* study of a human hepatoma cell line (Hep G2) showed the cellular membrane and mitochondria resistant to copper exposure, while the lysosomes interacted with the copper and were very susceptible to damage (Seth, *et al*., 2004:501). Also, cell viability was reduced the greatest (only 14 to 25 percent viability) after exposure to copper dental

alloys, as compared to other metals such as nickel, zinc, palladium, tin, and indium (Schmalz, *et al*., 1998:1693).

Copper Nanoparticles

Copper nanoparticles are used for many different industrial applications. Current usage includes lubricants, polymers, plastics, and metallic coatings and inks (Chen, Z., *et al*., 2006:110). Copper nanoparticles possess superior mending effects (Liu, G., *et al*., 2004:abstract). One study showed copper nanoparticles effectively decreased wear and friction and mended worn surfaces when used as oil additive (Tarasov, *et al*., 2002:69). Copper nanoparticles have also been used as a bimetallic catalyst on activated carbon effectively reducing elevated levels of nitrate in water (Barrabes, *et al*., 2006:84). Chen and Hong showed that the addition of 15 or 30 nm copper nanoparticles greatly increased the ductility of diamond-like carbon (DLC) nanocomposite films (2005:269). Copper nanoparticles have also been used in electrically conductive polymer composites as fillers (Zhang, *et al*., 2007). Also, the varying uses for copper nanoparticles extend beyond industrial applications.

Copper already is known as an effective antibacterial agent due to its ability to combine with the –SH enzyme group and lead to protein inactivation (Yoon, *et al*., 2007:572). One recent study evaluated the use of copper nanoparticles (100 nm) as antibacterial agents against *Escherichia coli* and *Bacillus subtilis*. The *B. subtilis* showed the greatest susceptibly when exposed to the copper nanoparticles; 31.37 µg/mL of copper nanoparticles degraded 90 percent of the *B. subtilis*, while 40.11 µg/mL was required to degrade the same percentage of *E. coli* (Yoon, *et al*., 2007:572 and 574). In

addition, copper-fluoropolymer (Cu-CFx) nano-composite films layers have been effectively utilized as a bioactive coating to inhibit microorganism growth to include *E. coli*, *Lysteria*, and *Staphylococcus aureus* (Cioffi, *et al*., 2005:607).

Different methods of producing copper nanoparticles have been utilized. Techniques used to create copper nanoparticles include the solvated metal atom dispersion (SMAD) technique (Ponce and Klabunde, 2005:1). Copper nanoparticles have also been plated on carbon nanotubes using an electroless plating method (Xu, *et al*., 2004:1499). Copper nanoparticles commonly possess a surface coating. If the particle does not contain a surface coating, it will most likely become oxidized when exposed to air. Athanassiou and colleagues discovered that copper nanoparticles with a carbon coating could be produced at up to 10 grams/hour by the use of a modified flame spray synthesis and under reducing conditions (2006:1668). Li and others sprayed copper nanoparticles with carbon-and-hydrogen (CH) plasma produced from a hollow-cathode glow discharge (HCGD) (Li, C., *et al*., 2004:1866).

As stated, there has been few toxicity studies conducted on copper nanoparticles. However, one recent *in vivo* study examined the toxicity effects of copper particles (micro-sized (17 µm) and nano-sized (23.5 nm)) by oral gavage in mice (Chen, Z., *et al*., 2006:111). As mentioned previously, the surface area of nanoparticles are significantly greater than larger counterparts. As determined by the use of atomic force microscopy, the copper nanoparticles surface area was 295,000 cm^2/g as compared to 399 cm^2/g for the microsized copper particles (Chen, Z., *et al*., 2006:111). However, one potential limitation of nanoparticle toxicity studies is the tendency for nanoparticles to

agglomerate, which leads to the formation of larger (i.e., micro-sized) particles, in which nanoparticles are then not effectively studied. To ensure limited agglomeration, Chen and colleagues ensured all mice were dosed within 20 minutes of nanoparticle preparation to ensure minimal agglomeration (2006:110). In the study, mice were exposed to copper nanoparticle doses of 108 to 1080 mg/kg, while the micro-copper doses where significantly higher (i.e., >5,000 mg/kg) (Chen, Z., *et al*., 2006:111). The determined lethal dose-50 (LD_{50}) for the copper nanoparticles was 413 mg/kg (moderately toxic classification on the Hodge and Sterner Scale) while the micro-copper LD_{50} was significantly higher at >5,000 mg/kg (non-toxic classification on the Hodge and Sterner Scale) (Chen, Z., *et al*., 2006:112). In addition, the copper nanoparticles displayed a dose-dependency degradation of the renal proximal tubular cells within the kidney of the mice (Chen, Z., *et al*., 2006:114). In addition to the kidney, the established target organs included the liver and the spleen (Chen, Z., *et al*., 2006:109). The spleen as a target organ is important because of the vital role it plays in both the lymphatic and immune system.

An associated study by Meng and colleagues examined the reaction of both micro-and-nano copper particles. The study, "Ultrahigh Reactivity and Grave Nanotoxicity of Copper Nanoparticles," showed that copper nanoparticles deposited into renal tissues more efficiently than the micron sized copper particles (Meng, *et al*., 2007:596). Once inside the kidney, the copper nanoparticles are extremely active and showed a tendency to react with the gastric juice and be converted by the hydrochloric acid to the more toxic cupric ions with an associated increase in pH (Meng, *et al*.,

2007:596). Copper nanoparticles are also toxic to non-mammalian toxicity models, as shown in "Exposure to Copper Nanoparticles Causes Gill Injury and Acute Lethality in Zebrafish (*Danio rerio*)." 80 nm copper nanoparticles displayed a 48-hour Lethal Concentration$_{50}$ (LC_{50}) of only 1.5 mg/L, as the gill was the primary target organ (Griffitt, *et al*., 2007).

Respiratory System

The human respiratory system is one of the few organ systems in the human body in constant contact with the environment. The respiratory system consists of two main sections; the conducting airways and the alveoli. The conducting airways move air in-and-out of the lungs, while the alveoli are responsible for carbon dioxide and oxygen gas exchange with the capillaries. The human lung contains on the order of 300 million alveoli within the deepest portion of the lung making the alveoli extremely susceptible to environmental contaminants because of their large surface area. In general, the smaller a particle is, the deeper the penetration within the human lung. Thus, the small size of nanoparticles makes them extremely effective in reaching the alveoli of the respiratory system (Hoet, *et al*., 2004). The International Commission of Respiratory Protection Task Group states that 30 percent of 3 µm particles can reach the lung while 55 percent of 0.05 µm particles can (Bates, *et al*., 1966).

Macrophages.

Macrophages are located throughout the entire human body and aid in the defense against various pathogens. Macrophages, which can be stationary or mobile within an

organ system, are terminally differentiated monocytes that are part of the non-specific, or innate immune system and are normally located in connective tissue. As part of the initial response within the immune system, macrophages play a key role in phagocytosis of particulates. However, macrophages also play a key role in the specific immune system as antigen presenting factors for lymphocytes. Other responsibilities of macrophages include particle clearance and the recruitment and activation of other inflammatory cells (Dörger and Krombach, 2002:47).

Macrophages serve as the first line of defense and have the ability to migrate to sites of injury or inflammation. If successful, macrophages will phagocytize and eliminate pathogens and other foreign materials. However, if unsuccessful, an associated inflammatory response can result in swelling and tissue injury (Laskin and Laskin, 2001:112). In addition, macrophages are secretory cells that are able to produce proinflammtory and cytotoxic mediators to include reactive oxygen species (Laskin and Laskin, 2001:111). Phagocytosis attempts can also lead to the activation of signal transduction factors to produce various cytokines, growth factors, and eicosanoids (Dörger and Krombach, 2002:50).

There are different types of macrophages that exist within the respiratory system to include alveolar, peritoneal, and pleural macrophages. However, important differences between the macrophages exist (Dörger, *et al*., 2001a:208). In the respiratory system, alveolar macrophages can be considered the primary phagocytes as they serve as a first line of defense against inhaled particulates. Alveolar macrophages exist between the air and lung interface and are located within the alveolus and on the epithelial surface in the

alveolar surfactant film (Lehnert, 1992:17; Gardner, 1984; Dörger, *et al*., 2001b:65). Alveolar macrophages are highly mobile cells and are the only aerobically exposed macrophages (Paine III, *et al*., 2001:L1210; Dörger and Krombach, 2002:47). Alveolar macrophages are also more likely to respond to a pathogen if complement factors are present. For example, one study, reviewed by Dörger and Krombach, showed asbestos fibers triggered the formation of the chemoattractant C5a, which increased alveolar macrophage response (2002:48).

Macrophages of various species are used for *in vitro* studies, with many showing differences in response. For example, mouse macrophages are more sensitive to metal ions from dental biomaterials than are human macrophages (Wataha, *et al*., 1995:243). Rat alveolar macrophages are used in many *in vitro* toxicity studies to measure the cytotoxic effects of various chemicals and particulates; thus, the differences between human and rat alveolar macrophages must be examined. The clearance rate for human and rat alveolar macrophages differ; the clearance rate for human macrophages is an order of magnitude lower than rat alveolar macrophages, as reviewed by Dörger and Krombach (2002:48). However, larger alveolar macrophages are able to phagocytize and remove larger, longer particulates and fibers and a study by Krombach and colleagues showed that human alveolar macrophages were larger than rat alveolar macrophages. Using selective flow cytometric analysis of cell volume, human alveolar macrophages were > 21 μm in comparison to 13 μm for rat alveolar macrophages (1997:1261). Also, a difference in cellular products exists between human and rat alveolar macrophages. One *in vitro* study showed the inability of human alveolar macrophages to produce inducible

nitric oxide synthase (iNOS) and nitric oxide (NO) when stimulated with lipopolysacchardie (LPS) and/or interferon-γ (IFN- γ), while rat alveolar macrophages were able to produce iNOS (Jesch, *et al*., 1997:1297).

After a particulate is introduced into the alveolar space, alveolar macrophages attempt to engulf the particulate and produce inflammatory mediators. The normal clearance mechanism for particulates, termed the mucociliary escalator, is via the trachea and subsequently cleared in the esophagus (Lam, *et al*., 2004:131). However, various situations exist in which macrophages are unable to successfully clear all particles by the normal pathway. One difficulty is the extremely small size of the particles and increased quantity of particles. If particles are too small, the macrophages may not effectively locate the particles for attempted phagocytosis (Renwick, *et al*., 2001:124). In addition, too many particles for a macrophage to successfully clear is termed overload (Lehnert, 1992). If macrophages do experience particle overload, the particles may interact with epithelial cells and cross the interstitial membrane (interstitialization) after which the particles can no longer be cleared by the normal pathways (Donaldson, *et al*., 1998:553-554; Oberdörster, G., *et al*., 1992:196-198). As reviewed by Bermundez, *et al*., prolonged overload can even lead to the formation of pulmonary tumors in rats (2004:354). Impaired macrophage mobility and toxicity to the macrophage are other factors in unsuccessful particle clearance (Donaldson, *et al*., 1998:554). An *in vivo* study of rats showed reduced clearance of particles due to macrophage damage after exposure to various doses of titanium dioxide (TiO_2)(5, 50, and 250 mg/m^3) (Warheit, *et al*., 1997:10).

As mentioned previously, nanoparticles possess increased surface areas as compared to larger counterparts. As reviewed by Donaldson, *et al*., using particle volume as the main indicator, macrophage clearance typically becomes impaired at 60 μm^3 particle/macrophage (i.e., six percent of a typical macrophage volume) based on the assumption that all particles in the lung are evenly distributed (1998). However, the particle surface area has shown to be a more important factor than particle volume in impaired macrophage clearance (Oberdörster, G., *et al*., 1994:178). One study of ultrafine particles showed a slower clearance rate, increased retention time, and an increased transport to the pulmonary interstitium as compared to fine particles (Oberdörster, G., *et al*., 1994:178). Macrophage clearance of ultrafine particles (titanium dioxide (20 nm)) became impaired at only 2.6 percent of macrophage volume and caused the clearance half-time to increase eightfold, as compared to fine titanium dioxide (250 nm) (Oberdörster, G., *et al*., 1994:177).

Cytokines

Cytokines are peptides, proteins, or glycoproteins that actively play a role in intracellular signaling (Bondeson, 1997:131). The body produces various cytokines that are an integral part of the human immune system, but also those that regulate inflammation, apoptosis, and hematopoesis and promote cellular growth (House, 2001:abstract). Many cytokines control multiple actions within the body. Cytokines normally act on a local level and are removed from the blood circulation rather quickly (House, 1999:18). There is also great redundancy within the human body as different cytokines perform the same function (House, 1999:18). For example, TNF and IL-6 may

be similar, but each bind to different receptors, as receptors can be either membrane-bound or soluble molecules (House, 1999:18 and 20). Cytokine production and the inflammation response of the immune system typically involve alveolar macrophages. The inflammatory response is a natural defense mechanism of the human body against foreign particulate matter. However, increased and prolonged inflammation can cause significant damage. Two proinflammatory cytokines, both secreted by alveolar macrophages, are TNF-α and IL-6.

Tumor Necrosis Factor-α.

TNF-α acts through both autocrine and paracrine pathways to stimulate the release of other cytokines that play a key role in the inflammatory response by recruiting and activating various inflammatory species, including neutrophils (Driscoll, *et al*., 1997:1159). TNF-α also plays a cytotoxic role against some tumor cells *in vivo* (Feliciani, *et al*., 1996:302). ROS production is stimulated by TNF-α which also depletes cellular GSH (Mukhopadhyay, *et al*., 2006). TNF-α stimulates inflammatory species to release IL-6 (Laskin and Laskin, 2001:115), and stimulates IL-6 itself (Driscoll, *et al*., 1997:1159). Macrophages rapidly produce TNF-α when inflammatory stimuli are present (Laskin and Laskin, 2001:114). Overall, TNF-α acts as a protective factor in smaller doses, but plays a role as a hepatotoxic in larger doses (Laskin and Laskin, 2001:115).

Interleukin-6.

IL-6 stimulates the hepatic synthesis of acute-phase plasma proteins and also B-cells (Feliciani, *et al*., 1996:302). IL-6 is a proinflammatory mediator in the chronic inflammation response (i.e., strengthens the effects of other proinflammatory cytokines such as IL-1 and TNF-α), but also an anti-inflammatory agent during the acute response (Rubin, *et al*., 2007; Bondeson, 1997:131; Lemaire and Ouellet, 1996:475).

TNF-α and IL-6 Studies.

As reviewed by Driscoll *et al*., *in vitro* alveolar macrophage studies showed TNF-α production after exposure to various contaminants such as quartz, crocidolite and chrysotile, and coal dust (1997:1159). Copper coated titanium disks showed an increase in TNF-α production *in vivo* in rats up to 24 hours (Suska, *et al*., 2003:465). One study attempted to study the interactions of non-nano size zinc ($ZnCl_2$) and iron ($FeCl_3$) with nanoparticle carbon black. The relationship between $ZnCl_2$ and the nanoparticles produced a synergistic effect in the production of TNF-α, while $FeCl_3$ and nanoparticle carbon black did not (Wilson, *et al*., 2007:88). An *in vitro* study of peritoneal cavity macrophages showed non-soluble functionalized carbon nanotubes produced TNF-α and IL-6, while soluble functionalized carbon nanotubes did not (Dumortier, *et al*., 2006:1526). Also, exposure to chitosan-DNA nanoparticles in a human THP-1 macrophage cell line did not induce TNF-α or IL-6 production (Chellat, *et al*., 2005:7265). One study discovered an increased release of IL-6 and an accompanying inflammatory response when exposed to asbestos fibers (Lemaire, *et al*., 1996:475). In addition, as reviewed by Warheit, *et al*., both human and bovine alveolar macrophages

produced increased IL-6 levels after *in vitro* exposure to nano-sized C_{60} fullerenes (2004:122).

Cellular Assays

MTS Assay.

Mitochondria play a critical role in cellular functions by aerobic adenosine triphosphate (ATP) production (Hussain and Frazier, 2002:430). The MTS assay (Promega CellTiter 96 AQ_{ueous} One Solution Cell Proliferation Assay) uses a tetrazolium compound ([3-(4,5-dimethylthiazol-2-yl)-5-(3-carboxymethoxyphenyl)-2-(4-sulfophenyl)-2H-tetrazolium, inner salt; MTS[(a)]]) and an electron coupling reagent (phenazine ethosulfate; PES) to measure cell viability. The assay measures cell viability when the tetrazolium compound is bioreduced by viable cells to a colored formazan product (see Figure 3, below). The conversion in viable cells is done by nicotinamide adenine dinucleotide phosphate (NADPH) or nicotinamide adenine dinucleotide (reduced form) (NADH) produced by dehydrogenase enzymes. The formazan product is measured at 490 nm absorbance and is relative to the number of viable cells (CellTiter 96 AQ_{ueous} One Solution Cell Proliferation Assay Technical Bulletin).

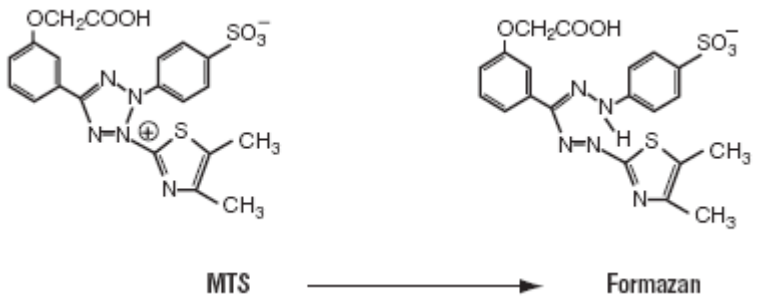

Figure 3. Chemical structure of MTS and the converted product of Formazan, which is a measure of cell viability (CellTiter 96 AQ_{ueous} One Solution Cell Proliferation Assay Technical Bulletin)

LDH Assay.

The CytoTox-ONE™ Assay evaluates the degree of damaged cellular membrane by measuring the amount of the enzyme lactate dehydrogenase (LDH) via a fluorescent measurement. As depicted in Figure 4 below, resorufin is measured after lactate, NAD+, and resazurin are supplied as substrates (CytoTox-ONE™ Homogenous Membrane Integrity Assay Technical Bulletin).

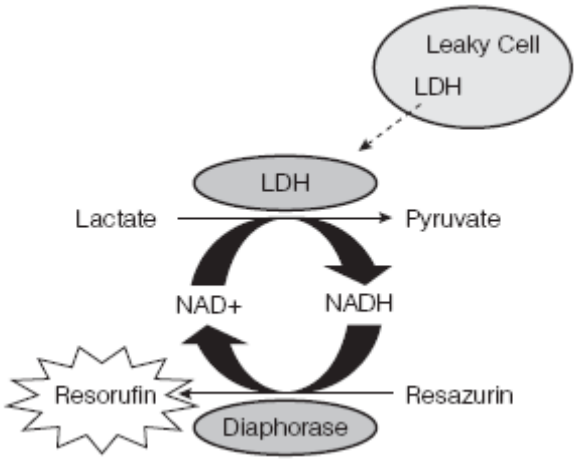

Figure 4. LDH Chemical Reaction (CytoTox-ONE™ Homogenous Membrane Integrity Assay Technical Bulletin)

ROS Assay.

The ROS procedure uses a 2',7'-dichlorofluorescein diacetate (DCFH-DA) probe. When applied to intact cells, DCFH-DA is enzymatically hydrolyzed to nonfluorescent DCFH or oxidized to dichlorofluorescein (DCF) if ROS are present. The DCF is then measured to approximate the degree of oxidative stress caused by ROS (Wang and Joseph, 1999:612-613).

Cytokine Assay.

An enzyme-linked immunosorbent assay (ELISA) is an immunoassay used to measure cytokine production. ELISA uses solid-phase antibodies able to extract a specific cytokine from a sample (i.e., cell culture supernatant). Another antibody is then used to convert a substrate to a colorimetric end product that can be measured by a plate reader (House, 2001:54).

III. Methodology

Overview

The methodology involved rat alveolar macrophages as the cell line for all *in vitro* toxicity and cytokine experiments. The progression of assays started with basic toxicity experiments (MTS and LDH), followed by mechanism of toxicity (ROS), and finally inflammation measurements (TNF-α and IL-6). For statistical significance, at least two to three separate experiments were done for each assay with multiple samples of each copper nanoparticle concentration. In addition, detailed experimental procedures are located in Appendices A through E.

Cell Culture

Frozen alveolar rat (*Rattus norvegicus*) macrophages were acquired from the American Type Culture Collection (ATCC). The cell line (ATCC Number: CRL-2192 and Designation NR8383) was initially isolated by lung lavage in August 1983. Some cellular products of the alveolar macrophages include transforming growth factor beta (TGF beta), interleukin 1 (IL-1), and interleukin 6 (IL-6) (ATCC).

F12K Medium Kaighn's Modification of Ham's F-12 with L-glutamine was used as the primary growth media. In addition, 20 percent fetal bovine serum (FBS) and one percent Penicillin/Streptomycin were added to the media. The growth media was stored at four degrees Celsius. Exposure media used included the above mentioned media and one percent Penicillin/Streptomycin, but only ten percent FBS.

Alveolar macrophages were maintained in 75 cm^2 plastic culture flasks (Corning Incorporated). Cell flasks were kept in an incubator at 37 degrees Celsius and five percent carbon dioxide (Thermo Electron Corporation Forma Series II Water Jacketed CO_2 Incubator). Macrophages were split into new culture flasks upon approaching a confluence of 50 percent. Cultures were maintained by scraping adherent cells with a plastic scraper (FisherBrand Disposable Cell Scraper) and then transferring cells to new culture flasks and periodically adding new growth media to the flasks.

Nanoparticle Solutions

Copper nanoparticles (40, 60, and 80 nm) were obtained from NovaCentrix (formerly Nanotechnologies, Inc.). Nanoparticle solutions were made by weighing out approximately two to four milligrams of nanoparticles on a balance (Denver Instrument Company) in a glass vial. Cadmium oxide particles (Fluka Chemicals, Sigma-Aldrich Corporation) were used as a positive control in the MTS assay, due to its highly toxic properties as shown in previous studies (Hussain, *et al*., 2005). Sterile millipore water was then added to the glass vial to make a one mg/mL stock solution for each size of copper nanoparticle. Each respective nanoparticle stock solution was then sonicated (Cole Palmer Instrument Co. Ultrasonic Homogenizer) for approximately 20 seconds to ensure proper particle suspension in solution and to reduce particle agglomeration. After sonication, each stock solution was used to make different doses (0 (just exposure media), 1, 2.5, 5, 7.5, and 10 µg/mL) of each respective copper nanoparticle (40, 60, and 80 nm) by dilution with the above described exposure media.

Experiment Overview

Each experiment included the following procedures: cell counting, cell plating, nanoparticle dosing, and the respective cellular assay. In total, five assays were performed, in order: MTS, LDH, ROS, TNF-α, and IL-6. The MTS assay was performed first to determine the appropriate particle concentrations that were toxic to alveolar macrophages.

Cell Counting.

Alveolar macrophages were counted before each experiment to ensure sufficient cells were available for each respective assay. Cells obtained from culture flasks were placed in 50 mL conical tubes and inverted twice to ensure adequate mixing of the cell suspension. 10 µL of cell suspension was then placed on a hemacytometer with a glass cover slip and placed under a microscope (Nikon Phase Contrast ELWD 0.3). The hemacytometer displays four equally sized quadrants that each contained 16 squares. Only cells within, on top, and to the left of each square were counted (i.e., cells on the right and bottom perimeter of each square were not counted). All cells were counted in each respective quadrant and then averaged over the four quadrants.

Cell Plating.

After cell counting, alveolar macrophages were plated at approximately 250,000 cells/mL in a 96-well clear bottom plate (Corning Incorporated Costar). Appropriate dilutions (i.e., $C_1V_1 = C_2V_2$) were performed using the cell suspension and growth

media. After the cells were plated, the 96-well plate was placed in the incubator (at conditions stated above) for 24 hours.

Nanoparticle Dosing.

After removing the 96-well plate from the incubator at the 24-hour time point, the growth media was aspirated (cells were adhered to the well bottom). Nanoparticle dosing solutions (prepared as described above in **Nanoparticle Solutions**) were vortexed (Fisher Scientific/Fixed Speed Mini Vortexer) for approximately five seconds directly before being added to each respective well to ensure a homogenous nanoparticle solution. The appropriate nanoparticle dosing solution (200 µL) was then added to each respective well in the 96-well plate and subsequently incubated for an additional 24 hours. As mentioned previously, as described by Z. Chen, *et al*. (2006), an effort was made to dose cells as rapidly as possible after sonicating, making dosing concentrations, and vortexing, to ensure minimal agglomeration of nanoparticles. Doses used included 1, 2.5 5, 7.5 and 10 µg/mL, depending on the specific experiment.

Cellular Assays

MTS Assay.

Following the procedures of Braydich-Stolle, *et al*. (2005), after incubation of dosed cells for 24 hours (see Figure 5, below), the exposure media containing the nanoparticle solutions were aspirated (cells were still adherent to the well bottom) and each well was rinsed three times with 200 µL of one percent phosphate buffered saline (PBS) (Invitrogen Corporation/10x Gibco Phosphate Buffered Saline, 7.2). 100 µL of

exposure media was then added to each well, followed by 20 µL of tetrazolium compound [3-(4,5-dimethylthiazol-2-yl)-5-(3-carboxymethoxyphenyl)-2-(4-sulfophenyl)-2H-tetrazolium, inner salt; MTS[(a)]] (Promega CellTiter 96 AQ_{ueous} One Solution Cell Proliferation Assay). The plate was then lightly tapped to ensure adequate mixing of the reagent within the cells attached to the plate. After a four hours incubation period at 37 degrees Celsius and five percent carbon dioxide, the plate was read on the Molecular Devices Spectra Max 190 plate reader at a wavelength of 490 nm. Three independent experiments were conducted with at least two separate samples (for each dosed concentration) for each experiment. The relative cell viability (%) results were computed by dividing the absorbance values from wells with dosed cells by the absorbance values from the control wells (i.e., wells with only macrophages and no nanoparticles). The two or more separate sample values were averaged as the mean of each independent experiment. The means of the three independent experiments values were subsequently taken as the overall relative cell viability (%).

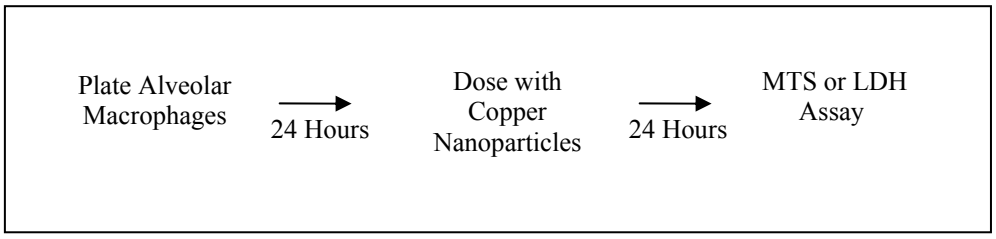

Figure 5. MTS/LDH assay procedures

LDH Assay.

Following the procedures of Braydich-Stolle, *et al*. (2005), the LDH assay (Promega CytoTox-ONE™ Homogenous Membrane Integrity Assay) was accomplished in conjunction with the above mentioned MTS assay. After incubation of dosed cells for

24 hours (see Figure 5, above), 50 μL of the supernatant from the 200 μL nanoparticle solution used for dosing was removed and placed in a new 96-well plate (50 μL of a positive control was also added to empty wells). 50 μL of reagent (CytoTox-ONE™) was then added to each well. The plate was then lightly shaken for approximately 30 seconds. This plate was incubated in the dark for 10 minutes at room temperature. Afterwards, 25 μL of stop solution was placed in each well and the plate was subsequently shaken for about 10 seconds. In addition, the plate was kept out of the direct light. Immediately following the stop solution addition, the fluorescent signal was measured in the Molecular Devices Spectra Max Gemini XS microplate reader, with an excitation wavelength of 560 nm and read at a wavelength of 590 nm. Three independent experiments were conducted with at least three separate samples (for each dosed concentration) for each experiment. The LDH leakage (%) results were computed by dividing the absorbance values from wells with dosed cells by the absorbance values from the control wells (i.e., wells with only macrophages and no nanoparticles). The three or more separate sample values were averaged as the mean of each independent experiment. The means of the three independent experiments values were subsequently taken as the overall relative cell viability (%).

Time Study.

After toxic effects were observed at the 24-hour time point, a time study using the MTS assay procedure described above was done with Cu-80 nanoparticles to determine cytotoxic effects at earlier time points (see Figure 6, below). The only difference was in the dosed cells incubation time. For the MTS assay described above, the incubation time

was 24 hours; however, during the time study, incubation times of dosed cells included one-, two-, three-, four-, six-, and eight-hour time intervals. One independent time study experiment was conducted with at least four separate samples for each dosed concentration. The four or more separate sample values were averaged as the mean of each independent experiment. The relative cell viability (%) results were computed by dividing the absorbance values from wells with dosed cells by the absorbance values from the control wells (i.e., wells with only macrophages and no nanoparticles). As only one separate experiment was conducted, the associated error was represented as the standard deviation of the four or more separate samples (as compared to the standard deviation of the means of each independent experiment as described in the MTS and LDH section). Thus, each dosed concentration had some associated error, as did the control.

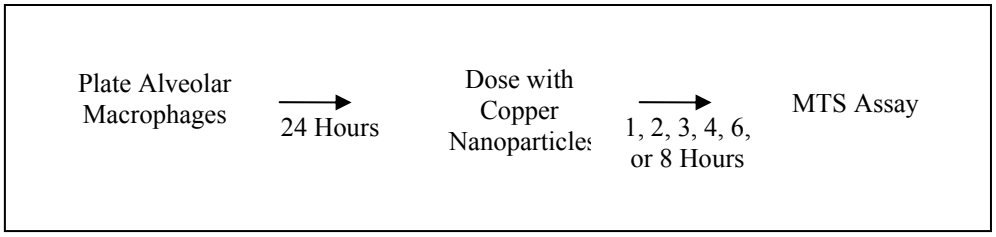

Figure 6. Time study procedures

ROS Assay.

Procedures were followed as described in Wang and Joseph (1999), only with minor modifications. For the ROS assay, a black bottom 96-well plate was used for the initial cell dosing, instead of a clear plate. After the 24-hour cell plating period, the growth media was removed and 200 µL of 100 µM dichlorofluorescin diacetate (DCFH-DA) probe was added to each well. The plate was then incubated at 37 degrees Celsius

and five percent carbon dioxide for 30 minutes. After the 30 minute incubation, the DFCH-DA probe was removed from each well and 200 μL of each respective nanoparticle solution was added to each well. In addition, a positive control of different molar strength (i.e., 100 to 2000 μM) hydrogen peroxide was used. The plate was then covered with aluminum foil and placed in the above mentioned incubator for different time exposures (i.e., 6 and 24 hours). At the 6-and-24 hour time points, the fluorescent signal was measured on the Molecular Devices Spectra Max Gemini XS microplate reader, with an excitation wavelength of 485 nm and read at a wavelength of 530 nm. During the entire assay procedure, all plates were treated in a dark room with only a fluorescent red light. Three independent experiments were conducted with at least three separate samples (for each dosed concentration) for each experiment. The ROS results were computed by dividing the fluorescent values from wells with dosed cells by the fluorescent values from the control wells (i.e., wells with only macrophages and no nanoparticles). The three or more separate sample values were averaged as the mean of each independent experiment. The means of the three independent experiments values were subsequently taken as the overall ROS fold of increase.

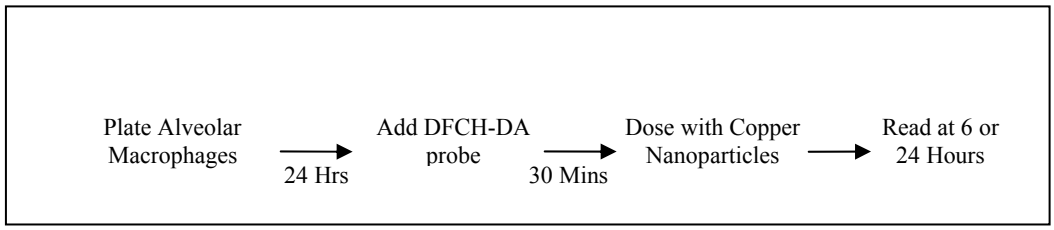

Figure 7. ROS procedures

TNF-α Assay.

The TNF-α Assay (R&D Systems, Inc. Catalog Number:DY510) was broken up into two separate steps. The first step was the ELISA plate preparation with the capture antibody. The second step consisted of adding a supernatant sample from a dosed plate to the prepared plate for determination of TNF-α production. The dosed plate was done as described in previous sections; however, a TNF-α stimulant was also used. The cellular activator used was *E. coli* lipopolysaccharide (LPS) (Sigma-Aldrich). House explains that for macrophages, the best cellular activator to use is LPS (1999:22). To determine what concentration was needed to stimulate TNF-α, a plate of LPS-dosed cells was done (i.e., no particles) before the actual experiment involving copper nanoparticles began.

To prepare the plate (Greiner Microlon LE High Binding Plates) during the first step, 100 µL of capture antibody (720 µg/mL of mouse anti-rat TNF-α reconstituted with 1.0 mL of PBS) was used to coat each well in a 96-well plate. After a 24-hour incubation period at room temperature, the capture antibody was aspirated and each well was washed with approximately 300 µL of wash buffer (Biosource 25x Wash Buffer) three times. The plates were then blocked by the addition of 300 µL of reagent diluent (one percent BSA (Calbiochem) in PBS) to each well. The plate was incubated at room temperature for one hour. After the one hour, the reagent diluent was aspirated and each well was washed as described above with the wash buffer. This concluded the first step of plate preparation.

After the plate was prepared, the second step began with adding 100 µL of the sample (i.e., supernatant from a dosed plate as described above) to each well in the prepared plate from the previously described step. The prepared plate with sample was covered with an adhesive strip and incubated at room temperature for two hours. After the two-hour incubation period, the plate was then aspirated and washed three times with the Wash Buffer used above. 100 µL of detection antibody (18 µg/mL of biotinylated goat anti-rat TNF-α when reconstituted with 1.0 mL of the described Reagent Diluent) was added to each well. The plate was covered with a new adhesive strip and incubated at room temperature for two additional hours. The aspiration and wash procedure as described above was used after the two-hour incubation period. 100 µL of Streptavidin-HRP (1.0 mL of streptavidin conjugated to horseradish-peroxidase) was then added to each well. The plate was covered and incubated at room temperature for 20 minutes. After the 20 minute period, the same aspiration and wash technique was used. 100 µL of substrate solution (1:1 mixture of Color Reagent A (H_2O_2) and Color Reagent B (Tetramethylbenzidine)) (KPL SureBlue Reserve TMB 1-Component Microwell Peroxidase Substrate) was then added to each well. The plate was incubated for 20 minutes at room temperature. 50 µL of stop solution (KPL TMB Stop Solution) was then added to each well and gently tapped to ensure mixing. Afterwards, the plate was immediately read on the Molecular Devices Spectra Max 190 plate reader set to 450 nm with a wavelength correction set to 540 nm.

Two independent experiments were conducted with two separate samples (for each dosed concentration) for each experiment. A standard curve was also developed

(recombinant rat TNF-α reconstituted with reagent diluent) to compare measured values against. The TNF-α production results were computed by comparing the absorbance values of each dosed sample to that of the developed standard curve. The two separate sample values were averaged as the mean of each independent experiment. The means of the two independent experiments values were subsequently taken as the overall TNF-α production.

IL-6 Assay.

The IL-6 Assay (R&D Systems, Inc. Catalog Number:DY506) was broken up into two separate steps. The first step was the ELISA plate preparation with the capture antibody. The second step consisted of adding a supernatant sample from a dosed plate to the prepared plate for determination of IL-6 production. The dosed plate was done as described in previous sections; however, a IL-6 stimulant was also used. The cellular activator used was *E. coli* lipopolysaccharide (LPS) (Sigma-Aldrich). House explains that for macrophages, the best cellular activator to use is LPS (1999:22). To determine what concentration was needed to stimulate IL-6, a plate of LPS-dosed cells was done (i.e., no particles) before the actual experiment involving copper nanoparticles began.

To prepare the plate (Greiner Microlon LE High Binding Plates) during the first step, 100 µL of capture antibody (720 µg/mL of mouse anti-rat IL-6 reconstituted with 1.0 mL of PBS) was used to coat each well in a 96-well plate. After a 24-hour incubation period at room temperature, the capture antibody was aspirated and each well was washed with approximately 300 µL of wash buffer (Biosource 25x Wash Buffer) three times. The plates were then blocked by the addition of 300 µL of reagent diluent (one

percent BSA (Calbiochem) in PBS) to each well. The plate was incubated at room temperature for one hour. After the one hour, the reagent diluent was aspirated and each well was washed as described above with the wash buffer. This concluded the first step of plate preparation.

After the plate was prepared, the second step began with adding 100 µL of the sample (i.e., supernatant from a dosed plate as described above) to each well in the prepared plate from the previously described step. The prepared plate with sample was covered with an adhesive strip and incubated at room temperature for two hours. After the two-hour incubation period, the plate was then aspirated and washed three times with the Wash Buffer used above. 100 µL of detection antibody (72 µg/mL of biotinylated goat anti-rat IL-6 when reconstituted with 1.0 mL of the described Reagent Diluent) was added to each well. The plate was covered with a new adhesive strip and incubated at room temperature for two additional hours. The aspiration and wash procedure as described above was used after the two-hour incubation period. 100 µL of Streptavidin-HRP (1.0 mL of streptavidin conjugated to horseradish-peroxidase) was then added to each well. The plate was covered and incubated at room temperature for 20 minutes. After the 20 minute period, the same aspiration and wash technique was used. 100 µL of substrate solution (1:1 mixture of Color Reagent A (H_2O_2) and Color Reagent B (Tetramethylbenzidine) (KPL SureBlue Reserve TMB 1-Component Microwell Peroxidase Substrate) was then added to each well. The plate was incubated for 20 minutes at room temperature. 50 µL of stop solution (KPL TMB Stop Solution) was then added to each well and gently tapped to ensure mixing. Afterwards, the plate was

immediately read on the Molecular Devices Spectra Max 190 plate reader set to 450 nm with a wavelength correction set to 540 nm.

Two independent experiments were conducted with two separate samples (for each dosed concentration) for each experiment. A standard curve was also developed (recombinant rat IL-6 reconstituted with reagent diluent) to compare measured values against. The IL-6 production results were computed by comparing the absorbance values of each dosed sample to that of the developed standard curve. The two separate sample values were averaged as the mean of each independent experiment. The means of the two independent experiments values were subsequently taken as the overall IL-6 production.

Dynamic Light Scattering

Copper nanoparticle stock solution samples (i.e., no exposure media) were placed in Cuvettes (Sarstedt Co.) and a Zetasizer® Nano (Malvern Instruments) machine to determine both average size and zeta potential. The purpose of DLS measurements is to determine the average size of nanoparticles in solution. The size advertised by the manufacturer (i.e., Cu-80 nanoparticles) may be the accurate size, but agglomeration of particles in powder form, and also within the stock solution (sterile water) or exposure media must be accounted for. Thus, DLS measurements must be made to determine nanoparticle size used in the dosing procedures. Measurements were taken in sterile water to give an accurate size measurement due to no presence of interferences such as proteins found in exposure media. In addition, concentrations of copper nanoparticles in exposure media were analyzed for size only in Zetasizer Nanoseries Folded Capillary

Cells (Malvern Instruments). (Note: zeta potential could not be determined for samples with exposure media due to conductivity incompatibilities within the Zetasizer® Nano). Measurements in exposure media were done to simulate conditions as to what size particle the cells were actually exposed to in exposure media. Finally, Mr. Michael Moulton (AFRL/RHPB) accomplished all DLS measurement analysis during my research.

Statistical Analysis

All statistical analysis was done in Microsoft Excel. After the completion of each respective assay, the results from the microplate reader were downloaded into Excel. The use of the Rejection Quotient, Q, was also used to determine outliers of data points after the completion of each independent experiment using a 95 percent confidence level (Rorabacher, 1991). Statistical significance was determined by using the students *t* test (two-sample assuming unequal variances, two-tailed analysis), also at a 95 percent confidence level.

IV. Results and Analysis

MTS Assay

Results of the MTS assay are expressed as the mean of at least two separate samples (± Standard Deviation) derived from three independent experiments. Statistical significance is indicated by an asterisk (*), based on $p < 0.05$ (using student's *t* test) compared to control (untreated) cells. The MTS assay showed that extremely low concentrations of all copper nanoparticles (Cu-40, 60, and 80) produced toxic conditions for rat alveolar macrophages. As seen in Figure 8 below, most cells were not viable after exposure to only 2.5 µg/mL of all sizes of copper nanoparticles tested. In fact, toxicity all sizes of copper nanoparticles was statistically significant as compared to the control (untreated) cells at 7.5 and 10 µg/mL. Only Cu-40 nanoparticles showed no statistically significant toxicity at 5 µg/mL. In addition, at 7.5 and 10 µg/mL, approximately only 20 percent of the alveolar macrophages were viable after exposure to all sized copper nanoparticles. As mentioned, micron sized cadmium oxide (CdO) was used as a positive control (results not shown) for each MTS experiment, because of its known toxic properties as determined in previous studies.

In general, Cu-80 nanoparticles were slightly more toxic than Cu-40 and Cu-60 nanoparticles, specifically at higher nanoparticle doses (i.e., ≥ 5 µg/mL). However, Figure 8 also shows that the toxicity of the copper nanoparticles was not size-dependent (no significant difference in toxicity between each sized copper nanoparticles), but was dose-dependent.

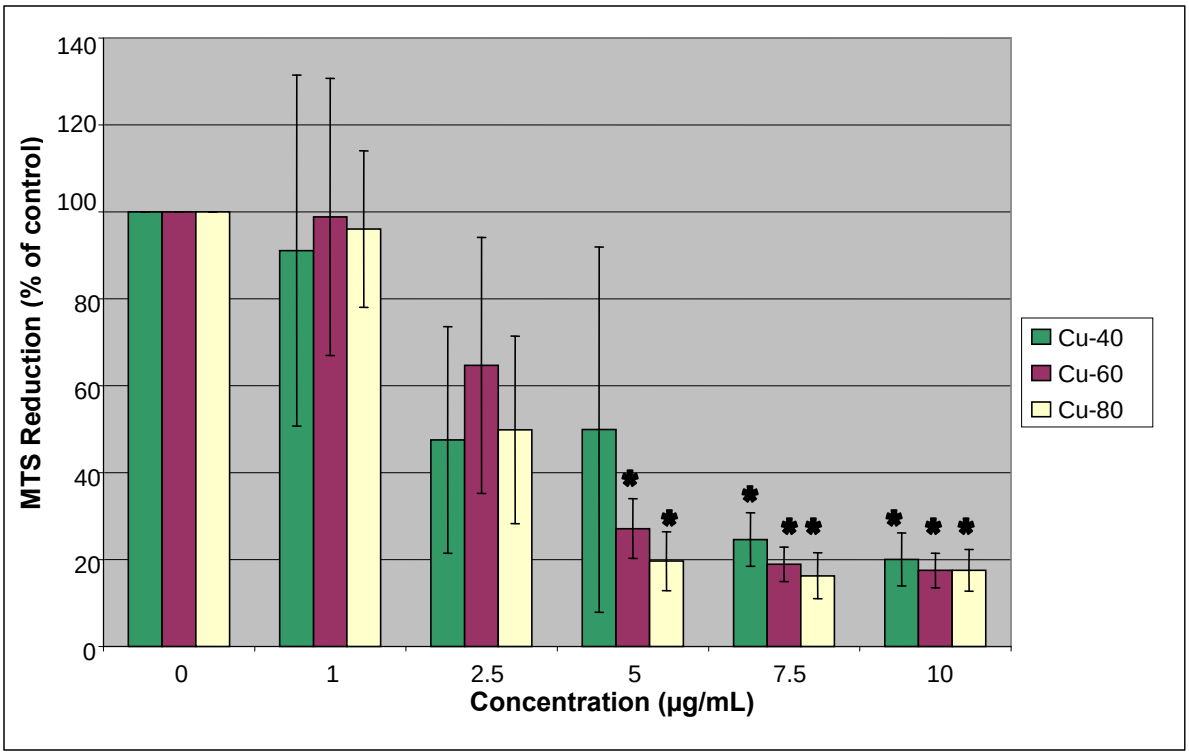

Figure 8. Combined MTS results (Cu-40, 60 and 80 nanoparticles)

Furthermore, since grave toxicity was seen after exposure to copper nanoparticles, it was assumed that alveolar macrophages would not survive and re-grow after a 24-hour time point; thus, longer time points (i.e., 48 or 72 hours) were not examined. However, since significant toxicity was seen at low copper nanoparticle concentrations at 24 hours, the next step was to determine if toxicity would be evident at earlier time points. Thus, a time study was conducted at time points to include one, two, three, four, six, and eight hours, as described below.

Time Study

Results of the time study are expressed as the mean of at least four separate samples (± Standard Deviation) derived from one experiment. Statistical significance tests were not accomplished due to only one independent experiment being conducted.

The time study used Cu-80 nanoparticles, primarily because of the time required to conduct this experiment (i.e., all copper nanoparticle sizes would not be feasible), and also because of the toxic properties described above (and below in the LDH analysis and discussion). Cu-80 nanoparticles were somewhat more toxic than Cu-40 and Cu-60 nanoparticles. Figure 9 below shows toxicity to Cu-80 nanoparticles as early as three and four hours, but only at significantly higher concentrations. Toxicity was also evident at a time point of six hours even at lower nanoparticle concentrations. However, some possible stimulation of cells at lower doses of Cu-80 nanoparticles was also observed (i.e., MTS reduction above 100 percent).

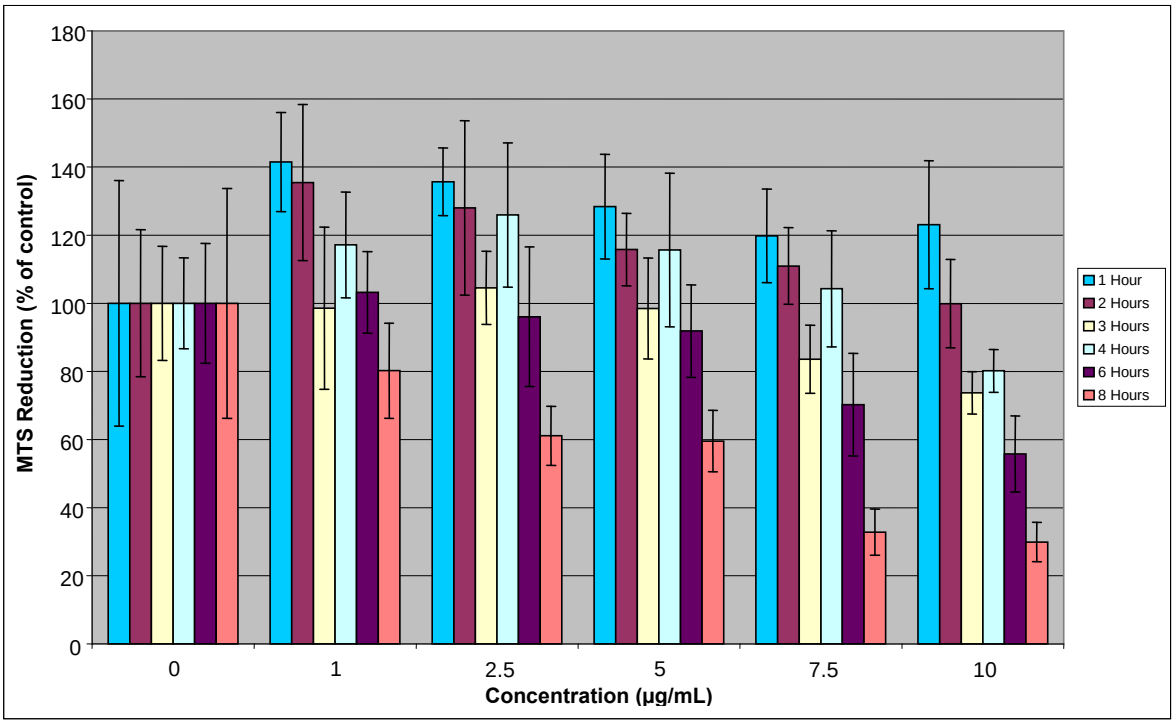

Figure 9. Cu-80 nanoparticle time study (≤ 8 hours)

LDH Assay

Results of the LDH assay are expressed as the mean of at least three separate samples (± Standard Deviation) derived from three independent experiments. Statistical significance is indicated by an asterisk (*), based on $p < 0.05$ (using student's *t* test) compared to the control (untreated) cells. The LDH assay showed a tremendous increase in membrane leakage in a dose-dependent manner. In addition, the LDH experiments, as did the MTS assay, showed that a significant size-dependent toxic effect between the different copper nanoparticles did not exist. However, of the three copper nanoparticles, Cu-80 showed the most membrane leakage, as compared to Cu-40 and Cu-60 nanoparticles. As seen in Figure 10 below, toxicity of all copper nanoparticles was statistically significant at 5, 7.5, and 10 µg/mL as compared to the control (untreated) cells. Consequently, the large degree of membrane leakage in dose-dependent concentrations from 1 to 10 µg/mL indicated that cellular necrosis occurred; cellular apoptosis would have a weaker response in membrane leakage.

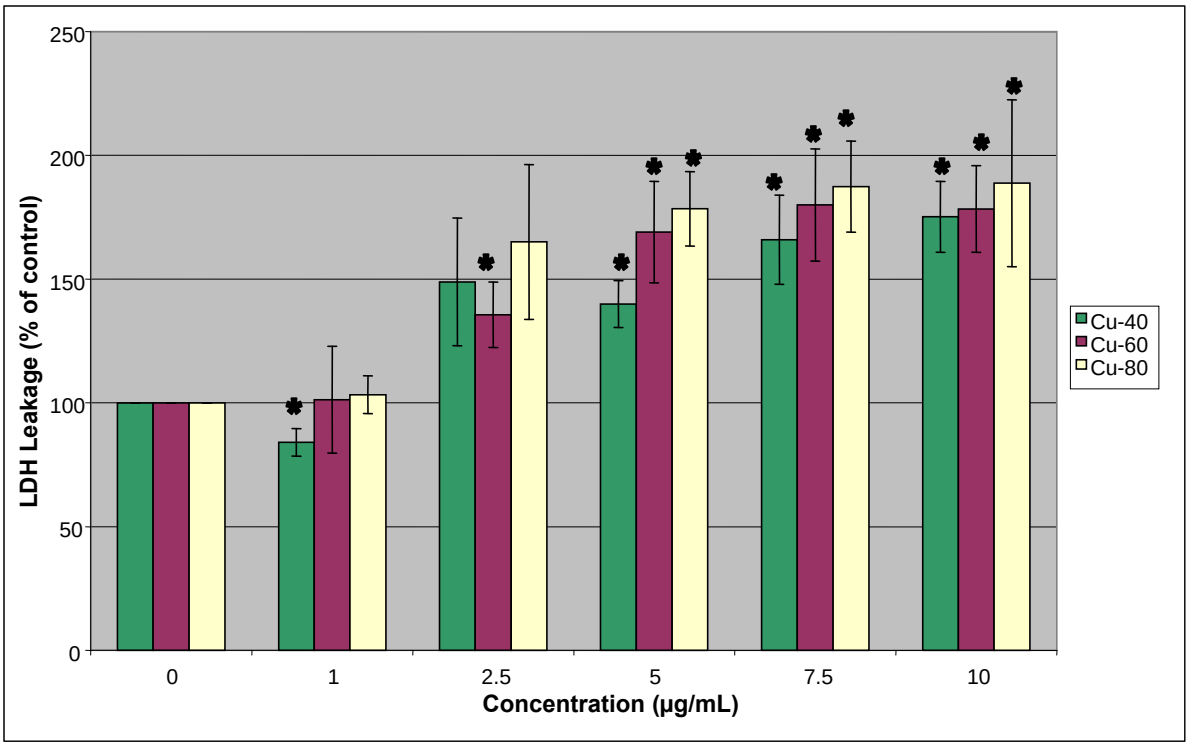

Figure 10. Combined LDH results (Cu-40, 60 and 80 nanoparticles)

An additional goal of the MTS and LDH experiments was to determine what concentrations to use for further experiments to include the two cytokine ELISA kits (TNF-α and IL-6). The MTS and LDH experiments showed that severe toxicity was evident at 5 µg/mL (see Figures 8 and 10, above). Thus, further experiments focused on copper nanoparticle doses ≤ 5 µg/mL (i.e., 1, 2.5, and 5 µg/mL), primarily because a measurement of a specific cytokine production would be limited to viable macrophages.

Reactive Oxygen Species

Results of the ROS experiments are expressed as the mean of at least three separate samples (± Standard Deviation) derived from three independent experiments. Statistical significance is indicated by an asterisk (*), based on $p < 0.05$ (using student's *t* test) compared to control (untreated) cells.

Overall, only a slight increase in ROS production was observed, indicating oxidative stress was not a significant mechanism of toxicity. General observations include ROS production at the 6-hour time point greater than the 24-hour time point, especially for Cu-80 nanoparticles (see Figure 13, below). However, as indicated in the LDH analysis, large degrees of membrane leakage led to cellular necrosis and an associated cellular leakage of the fluorescent product. This phenomenon could cause greater time points (24 hours and large degrees of associated membrane leakage) to have less ROS production than some lesser time points (6 hours). Also, the intensity of the DFCH-DA probe could have decreased at the 24-hour time point and caused less ROS production. In addition, with Cu-80 nanoparticles, the ROS production actually decreased at the highest concentration of 10 µg/mL (see Figure 13, below); this phenomenon can be attributed to the same cellular leakage indicating a decreased ROS production (Hussain and Frazier, 2002:430). No measurement points were statistically significant at the 24-hour time point, as compared to control (untreated) cells (see Figures 11, 12, and 14, below), except for the 1 and 10 µg/mL Cu-80 measurement points (see Figure 13, below). However, statistically significant differences did exist at the 6-hour time point to include both the 5 and 10 µg/mL exposure points for the Cu-40 exposure (see Figure 11, below). In fact, most Cu-80 nanoparticles exposures (1, 2.5, 5, and 10 µg/mL) produced statistically significant differences at the 6-hour time point (see Figure 13, below). As seen in Figure 12 below, Cu-60 nanoparticles showed a large increase at 10 µg/mL; however, the standard deviation was extremely large, indicating a potential measurement error.

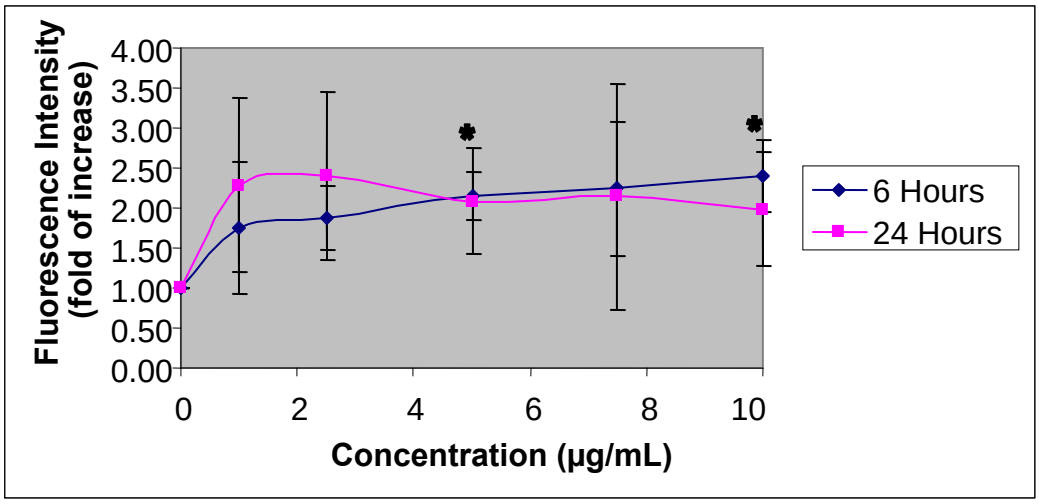

Figure 11. ROS production at 6 and 24 hours after exposure to Cu-40 nanoparticles

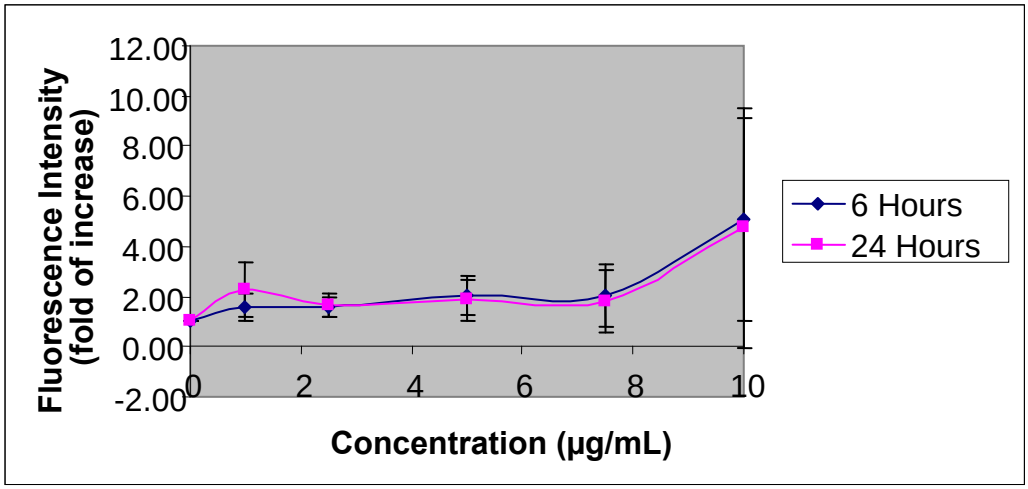

Figure 12. ROS production at 6 and 24 hours after exposure to Cu-60 nanoparticles

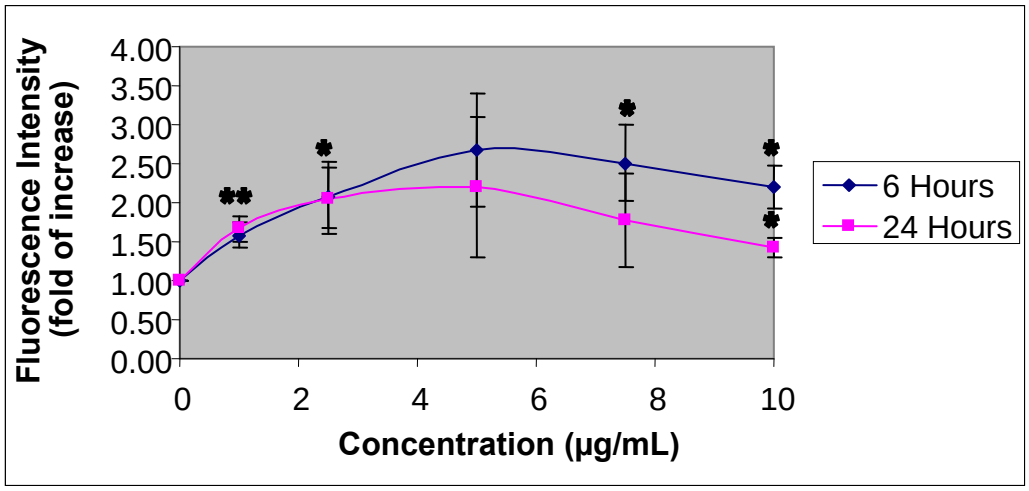

Figure 13. ROS production at 6 and 24 hours after exposure to Cu-80 nanoparticles

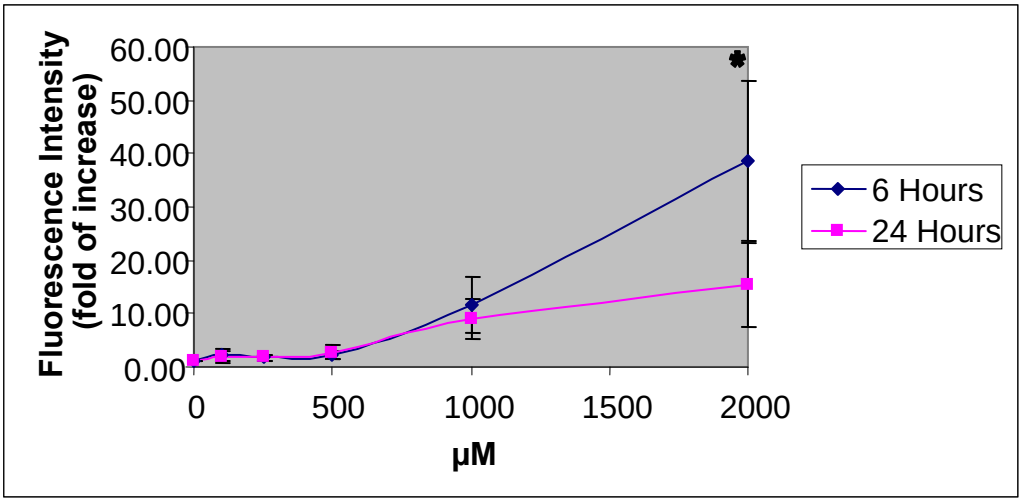

Figure 14. ROS production at 6 and 24 hours after exposure to Positive Control (hydrogen peroxide)

Although the positive control (hydrogen peroxide) for the 6-and-24 hour time points showed a large increase in ROS production (see Figure 14, above), a greater increase was expected in response to copper nanoparticles exposure due to previous ROS experiments from the AFRL toxicological laboratory (unpublished data) using copper nanoparticles (used PC12 cells as *in vitro* model). In addition, Ag (15-nm) nanoparticles

induced ROS production fold of increases greater than six at 10 µg/mL (Hussain, et al., 2005:980). After performing ROS experiments and further investigation, it was brought to my attention that exposure media containing phenol-red may influence and weaken actual increases in ROS production. Thus, ROS experiments were performed again using exposure media not containing phenol-red as my original ROS experiments used exposure media with phenol-red. Surprisingly, lower increases in ROS production were observed when using the phenol-red free exposure media (results not shown).

Cytokine Analysis

The first step in optimizing each cytokine assay (TNF-α and IL-6) was development of a standard curve (using recombinant rat TNF-α or IL-6 reconstituted with Reagent Diluent, as described above in the **Methodology** section). The standard curve using the four-parameter method produced R^2 values of ≥ 0.98, indicating a highly precise curve. The next step was to determine if copper nanoparticles induced TNF-α or IL-6 production. If the copper nanoparticles did not induce cytokine production, the next step was to determine a LPS concentration to stimulate alveolar macrophage production of TNF-α or IL-6. The goal was to find an LPS concentration that would produce each cytokine in suboptimal amounts. The LPS would be used as an agent to stimulate cells while being exposed to copper nanoparticles. Exposing cells to LPS in the presence of another chemical has been previously done. One experiment stimulated murine macrophages with LPS while concurrently exposing the cells to mycophenolic acid to measure TNF-α production (Jonsson and Carlsten, 2002:94). Other studies have used the same approach (Major, *et al*., 2002:2457). The difference in cytokine production

between the LPS stimulated cells alone and LPS + copper nanoparticle exposed cells would be calculated to be the amount of cytokine production due to copper nanoparticle exposure.

Summary of Cytokine Steps:

- Standardize plates with TNF-α and IL-6 standards (Note: a standard curve was developed for every experiment to account for potential errors between various plate preparations)
- Determine if copper nanoparticles induced cytokine production in alveolar macrophages
- If copper nanoparticles did not induce cytokine production, determine LPS concentrations to produce suboptimal amounts of each cytokine
- Determine cytokine production due to copper nanoparticles by stimulating alveolar macrophages with LPS followed by exposure to copper nanoparticles

LPS also was used a positive control to indicate cytokine production as compared to copper nanoparticle exposed cells only (i.e., not using LPS).

TNF-α Analysis.

Results of the TNF-α assay are expressed as the mean of two separate samples (± Standard Deviation) derived from two independent experiments. Statistical significance is indicated by an asterisk (*), based on $p < 0.05$ (using student's *t* test) compared to LPS treated cells. For the exposure to copper nanoparticles only (see Figure 15, below), there was no statistically significant differences in TNF-α production as compared to control (untreated) cells at concentrations of 1, 2.5, or 5 µg/mL. As mentioned above, LPS was

used as a positive control to indicate TNF-α production (see Figure 16, below), while exposure to copper nanoparticles did not produce TNF-α release. Thus, the next step was to determine varying concentrations of LPS to stimulate alveolar macrophages to produce TNF-α before subsequent exposure to copper nanoparticles.

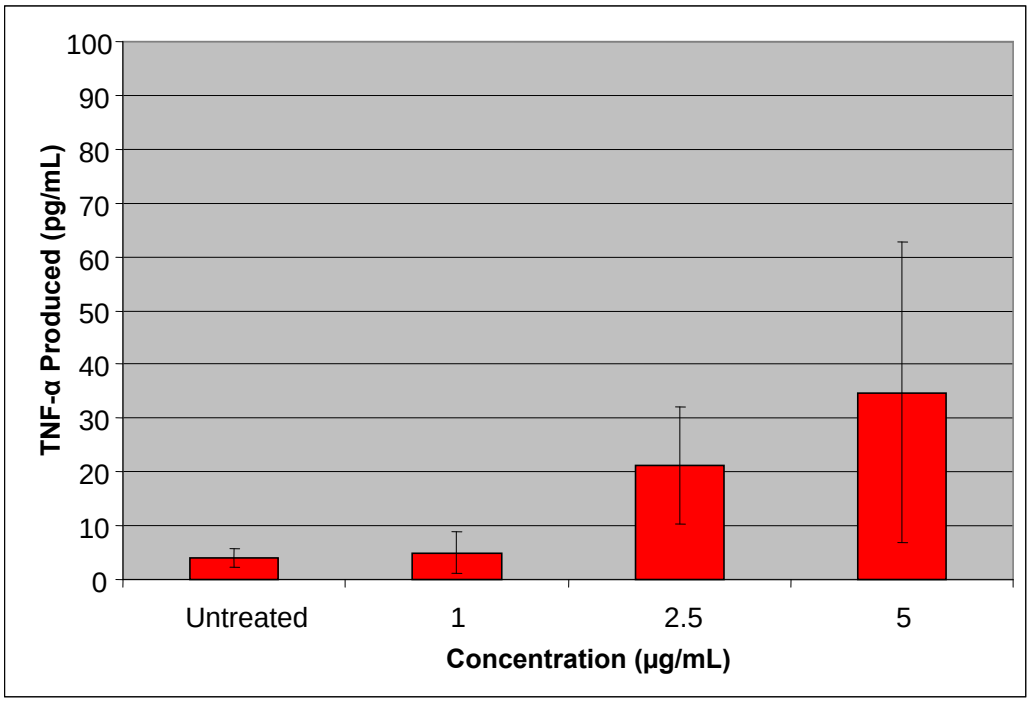

Figure 15. TNF-α produced after exposure to Cu-80 nanoparticles

For the TNF-α cytokine experiment, 0.1 ng/mL was determined to be the suboptimal concentration (over a 24-hour time period) of LPS (an initial experiment showed that as low as 25 ng/mL released excess amounts of TNF-α). 0.1 ng/mL of LPS over a 24-hour time period showed production of approximately 50 pg/mL (see Figure 16, below). Dumortier and colleagues showed levels > 6000 pg/mL of TNF-α production by macrophages (isolated from the peritoneal cavity) in response to 8 ng/mL of LPS for a 24-hour time period (2006:1526). Other studies used as much as 10 µg/mL of LPS for an

ideal response from both human and rat alveolar macrophages (McRithie, *et al*., 2000:646 and Losa Garcia, *et al*., 1999:49). Another experiment using the same cell line of this research (rat alveolar macrophages (NR8383)), and the same R&D Systems ELISA kit, showed that a 24-hour LPS exposure (100 ng/mL) produced approximately 10,545 pg/mL of TNF-α. However, Y. Li and colleagues (2000) used more cells (1,000,000 cells/mL) as compared to these experiments (250,000 cells/mL), indicating that more cells could potentially produce higher levels of cytokines. Another study showed 5,200 pg/mL of TNF-α was produced (using same rat alveolar macrophage (NR8383) cell line) after exposure to one µg/mL of LPS for 20 hours (Diabaté, *et al*., 2002:325). However, ELISA techniques were not utilized and the author also did not indicate how many cells/mL were initially plated (Diabaté, *et al*., 2002:324).

The production of TNF-α increased in a dose-dependent manner (after stimulated with LPS), with 5 µg/mL concentrations producing the highest amount of TNF-α. This was evident as exposure to Cu-80 nanoparticles was statistically significant at a 2.5 µg/mL concentration. TNF-α production was also statistically significant at 2.5 and 5 µg/mL exposure to Cu-60 nanoparticles. Also, as seen in Figure 16 below, the greatest production of TNF-α (approximately 500 pg/mL above the LPS only exposure) was seen after exposure to Cu-80 nanoparticles, as some size dependency was seen in TNF-α production.

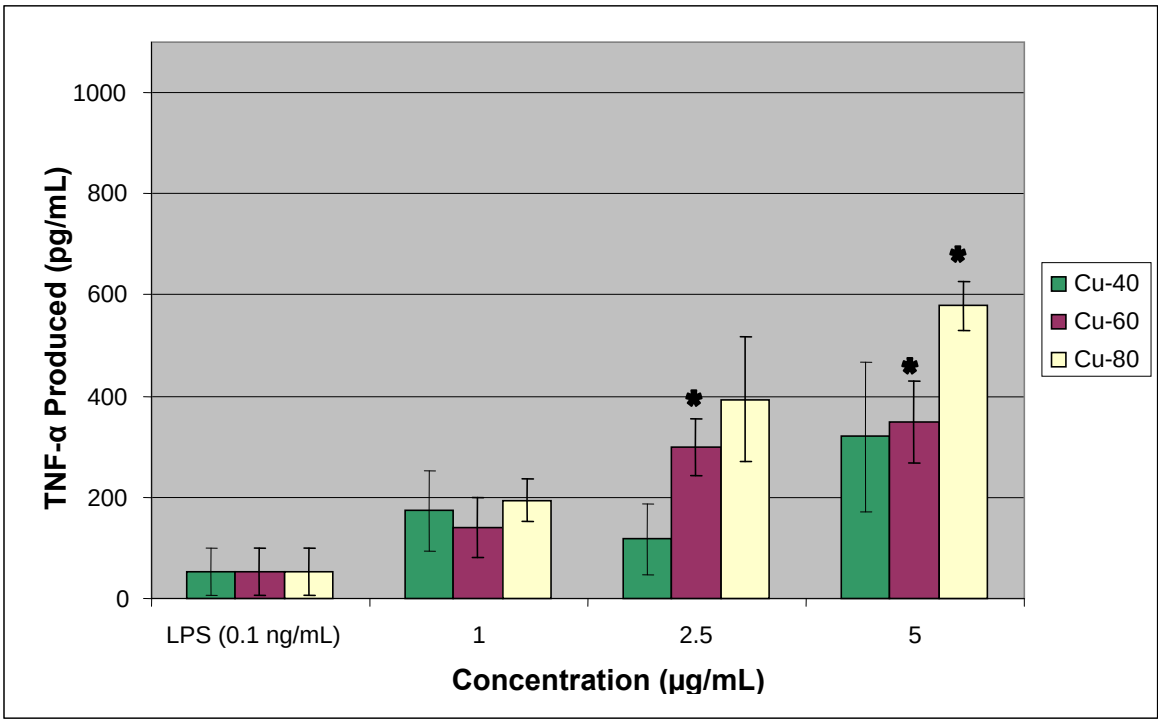

Figure 16. Combined (Cu-40, 60, 80 and LPS) results of TNF-α produced

IL-6 Analysis.

Results of the IL-6 are expressed as the mean of two separate samples (± Standard Deviation) derived from two independent experiments. Statistical significance is indicated by an asterisk (*), based on $p < 0.05$ (using student's *t* test) compared to LPS treated cells. As was the case with TNF-α production, Cu-80 nanoparticles did not stimulate a statistically significant amount of IL-6 production (results not shown) at concentrations of 1, 2.5 or 5 µg/mL. The amount produced after exposure to Cu-80 nanoparticles was essentially equivalent to the zero dose. As mentioned above, LPS was used as a positive control to indicate cytokine production (see Figure 17, below), while exposure to copper nanoparticles did not produce IL-6 release. Thus, the next step was to determine a LPS concentration to stimulate alveolar macrophages to produce suboptimal

amounts of IL-6. For the IL-6 cytokine experiment, 100 ng/mL was determined to be the suboptimal concentration (over a 24-hour time period) of LPS to be used during subsequent experiments to stimulate alveolar macrophages. 100 ng/mL of LPS over a 24-hour time period showed production of approximately 5,160 pg/mL (see Figure 17, below). Dumortier and colleagues showed levels > 100,000 pg/mL of IL-6 production by macrophages (isolated from the peritoneal cavity) in response to 8 ng/mL of LPS for a 24-hour time period (2006:1526). Another study using the same cell line as this research (rat alveolar macrophages (NR8383)) and the same R&D Systems ELISA kit, showed that a 24-hour LPS exposure (100 ng/mL) produced approximately 62,400 pg/mL of IL-6. However, in the Y. Li and colleagues (2000) experiment, more cells (1,000,000 cells/mL) were used as compared to my experiments (250,000 cells/mL), indicating that more cells could potentially produce higher levels of cyokines.

Figure 17, below, shows that most copper nanoparticle concentrations induced the production of IL-6 after initial LPS stimulation; however, only Cu-60 and Cu-80 nanoparticles (at 2.5 µg/mL) produced a statistically significant difference between the LPS stimulated cells (100 ng/mL). Exposure to Cu-60 nanoparticles (at 2.5 µg/mL) induced the highest amount of IL-6 production at approximately 2 ng/mL above the LPS alone exposure. All copper nanoparticles showed an increase in IL-6 production from 1 to 2.5 µg/mL concentrations, but a decrease in IL-6 production from the 2.5 to 5 µg/mL concentrations. Also, after conducting a preliminary IL-6 experiment, higher copper nanoparticle concentrations produced lower levels of IL-6. For example, 10 µg/mL produced lower amounts of IL-6 then at 5 µg/mL (results not shown). This indicated, and

was supported by the above MTS viability study, that at 10 µg/mL, and to some degree at 5 µg/mL, most of the cells were not viable and unable to release IL-6. Thus, copper nanoparticles concentrations less than 5 µg/mL induced higher levels of IL-6. This phenomenon of separating cellular toxicity from cytokine production was also described by Schmalz and others in a study of copper dental alloys in an *in vitro* study of human fibroblast-keratinocytes (1998). The study showed that copper exposure resulted in only 25 percent cell viability; thus, the cells would not be alive to produce inflammatory markers. Overall, the copper produced the pro-inflammatory markers, as measured by the production of IL-6, only at the lower levels of copper exposure (Schmalz, *et al*., 1998:1694).

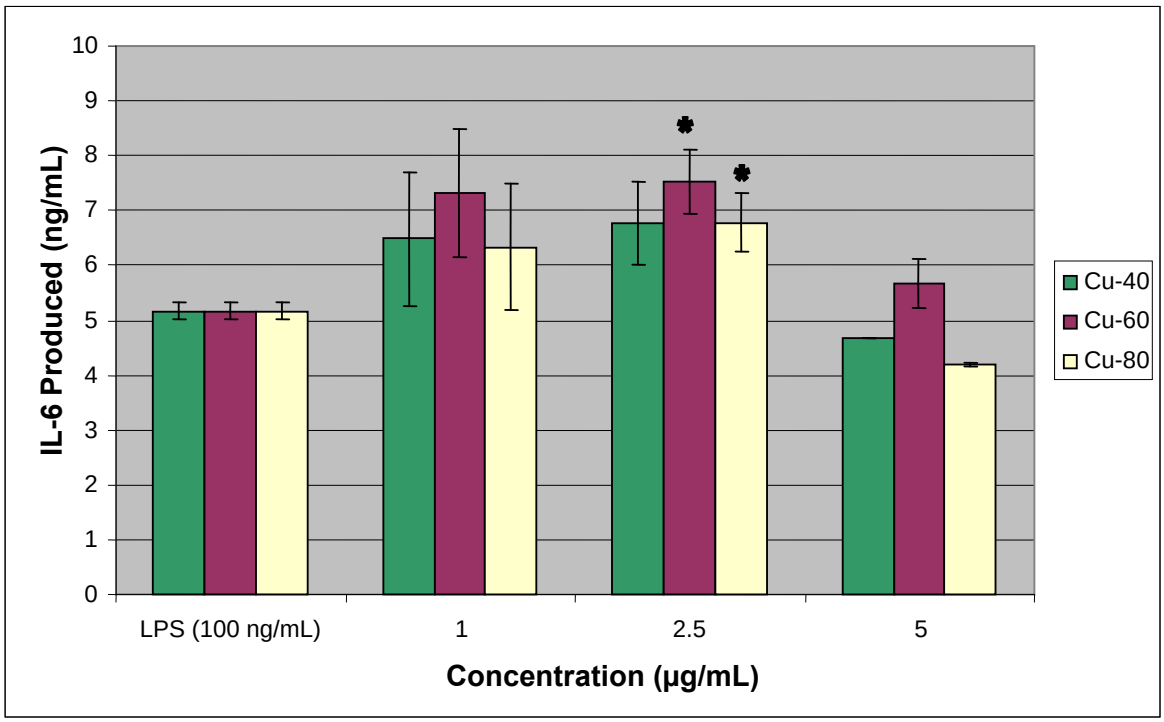

Figure 17. Combined (Cu-40, 60, 80 and LPS) results of IL-6 produced

Dynamic Light Scattering

Dynamic Light Scattering (DLS) results for 0 and 24 (Table 2) hours are below. Each table displays the average size, polydispersity index (PDI) and zeta potential of each copper nanoparticle. As mentioned in the **Methodology** section above, 0-and 24-hour time points were measured to determine differences in size over a 24-hour exposure period to macrophages. The results show that the average size of each copper nanoparticle is larger than the size given by the manufacturer. However, the size measured was the average size; thus, some particles could be the stated size (i.e., 40 nm for Cu-40 nanoparticles) while others agglomerated. In addition, as mentioned above, other interferences (i.e., presence of proteins in exposure media) could be present that influence the average reading size.

Table 2. DLS results, 0-and 24-hour time points

Sample Type	Average Size (nm)	PDI	Zeta Potential (mV)
Time Point	0 hr / 24 hr	0 hr / 24 hr	0 hr / 24 hr
40nm in Sterile H_2O	301 / 375	0.186 / 0.398	-13 / -2.78
40nm in Exposure Media	338 / 271	0.257 / 0.387	N/A / N/A
60nm in Sterile H_2O	321 / 582	0.185 / 0.508	-9.56 / -10.1
60nm in Exposure Media	329 / 283	0.236 / 0.381	N/A / N/A
80nm in Sterile H_2O	358 / 570	0.214 / 0.537	-7.07 / -12.9
80nm in Exposure Media	322 / 310	0.219 / 0.406	N/A / N/A

V. Discussion

Nanomaterials have numerous useful properties; however, further research on environmental and human health effects is needed. In fact, Material Safety Data Sheets (MSDSs) for most nanomaterials simply list the properties and safety and health precautions for the larger bulk material when the two can be entirely different (Colvin, 2003:1166). Overall, as nanoparticles show toxic effects to rodents, actual human exposure must also be considered.

Research Questions and Conclusions

- Are copper nanoparticles (40, 60, and 80 nm) toxic to alveolar macrophages?
    - All copper nanoparticles showed significant toxicity for rat alveolar macrophages. Concentrations as low as 2.5 μg/mL showed cell viability of less than 50 percent. Also, the same concentration showed membrane leakage increases of 50 percent. Concentrations of 10 μg/mL produced cell viability of less than 20 percent and membrane leakage increases of approximately 75 percent. Thus, the large dose-dependent increases in membrane leakage indicated cellular necrosis occurred, as opposed to apoptosis.
- Is the toxicity size-dependent (i.e., difference in toxicity between the three sizes of copper nanoparticles)?
    - Overall, there was no significant size dependency in toxicity between the three copper nanoparticles (40, 60, and 80 nm); however, the observed toxicity was dose-dependent.

- Do copper nanoparticles induce reactive oxygen species (ROS)?
    - Overall increases in ROS were low (only 2.5 fold increases) compared to other studies involving nanoparticles, indicating low levels of oxidative stress.
- Do copper nanoparticles induce an inflammatory response (using cytokines TNF-α and IL-6 as indicators)?
    - The results from the cytokine ELISA analysis show that copper nanoparticles do not produce an inflammation response. However, when stimulated initially (i.e., using LPS), exposure to copper nanoparticles did produce increased levels of both TNF-α and IL-6.

Suggestions for Further Research

As mentioned, one *in vivo* experiment has been conducted with copper nanoparticles (Chen, Z., *et al*., 2006). However, this experiment focused on ingestion exposure; thus, further *in vivo* studies focusing on inhalation exposures are needed. Also, a time study of all sizes of copper nanoparticles is needed (i.e., Cu-40 and Cu-60), as this research focused on Cu-80 nanoparticles. A potential experiment involving the cytokine ELISA (TNF-α and IL-6) kits would be to determine what response alveolar macrophages, or other immune cell types, would have to a physiological stimulus (i.e., LPS) after exposure to copper nanoparticles and a set incubation period. Similar research was conducted by Dumortier and colleagues using functionalized carbon nanotubes (2006). In addition, to more effectively identify a LPS concentration to stimulate alveolar macrophages to produce suboptimal concentrations of a specific cytokine, a time study at time points less than 24 hours could be conducted. Also, another potential

concern is the toxicity associated with LPS exposure to induce cytokine production (Diabaté, *et al*., 2002). Thus, a side-by-side study could also examine the toxicity associated with exposure to LPS while performing the specific ELISA analysis. Also, transmission electron microscopy (TEM) studies have been accomplished on all sizes of copper nanoparticles; however, no scanning electron microscopy (SEM) images, showing the potential uptake of copper nanoparticles by rat alveolar macrophages, have been accomplished. Finally, further research of the characterization of copper nanoparticles will be of benefit in further biochemical studies.

Appendix A. MTS Assay Protocol

1. Aspirate exposure media containing nanoparticle solutions (cells still adherent to the well bottom)
2. Rinse each well three times with 200 μL of one percent Phosphate Buffered Saline (PBS)
3. Add 100 μL of exposure media to each well
4. Add 20 μL of tetrazolium compound [3-(4,5-dimethylthiazol-2-yl)-5-(3-carboxymethoxyphenyl)-2-(4-sulfophenyl)-2H-tetrazolium, inner salt; MTS[(a)]] to each well
5. Lightly tap the plate to ensure adequate mixing of the reagent within the cells
6. Incubate plate for one to four hours at 37 degrees Celsius and five percent carbon dioxide
7. Read the plate on the Molecular Devices Spectra Max 190 plate reader at a wavelength of 490 nm

Appendix B. LDH Assay Protocol

1. Add 50 µL of the supernatant from the 200 µL nanoparticle solution used for dosing and place in a new 96-well plate
2. Add 50 µL of a positive control to empty wells
3. Add 50 µL of reagent (CytoTox-ONE™) to each well (supernatant and positive control wells)
4. Lightly shake the new plate for approximately 30 seconds
5. Incubate plate in the dark for 10 minutes at room temperature
6. Add 25 µL of stop solution to each well
7. Lightly shake the plate for about 10 seconds
8. Immediately after adding stop solution, measure the fluorescent signal in the Molecular Devices Spectra Max Gemini XS microplate reader, with an excitation wavelength of 560 nm and read at a wavelength of 590 nm

Note: Keep plate out of the direct light

Appendix C. Reactive Oxygen Species Protocol

1. Use black bottom 96-well plate for the initial cell dosing instead of a clear plate
2. After the 24-hour cell plating period, remove growth media and add 200 μL of 100 μM dichlorofluorescin diacetate (DCFH-DA) probe to each well
3. Incubate plate at 37 degrees Celsius and five percent carbon dioxide for 30 minutes
4. Remove DFCH-DA probe from each well
5. Add 200 μL of each respective nanoparticle solution to each well
6. Use a positive control of different molar strength (i.e., 100 to 2000 μM) hydrogen peroxide
7. Cover plates with aluminum foil and place in incubator for different time exposures (i.e., 6 and 24 hours)
8. Measure fluorescent signal on the Molecular Devices Spectra Max Gemini XS microplate reader, with an excitation wavelength of 485 nm and read at a wavelength of 530 nm

Note: Treat in a dark room with only a fluorescent red light

Appendix D. TNF-α ELISA Protocol

(Catalog Number: DY510 (R&D Systems, Inc.)

Materials and solutions required:

- **ELISA plates** - Greiner Microlon LE High Binding Plates
- **Phosphate Buffered Saline**
- **Wash Buffer** - Biosource 25X Wash Buffer (WB01/Q110408)) – diluted with deionized water to 1X
- **Reagent Diluent** - 1% BSA Calbiochem (Cat#12659) in PBS
- **Substrate Solution** - KPL SureBlue Reserve TMB 1-Component Microwell Peroxidase Substrate (Cat #:53-00-03)
- **Stop Solution** – KPL TMB Stop Solution (Cat#:50-85-05)
- **Stimulant** - Lipopolysaccharide (LPS): Sigma-Aldrich (Cat#:L2630)
- **Capture Antibody** - 720 µg/mL of mouse anti-rat TNF-α when reconstituted with 1.0 mL of PBS. Dilute to a working concentration of 4.0 µg/mL in PBS, without carrier protein.
- **Detection Antibody** - 18 µg/mL of biotinylated goat anti-rat TNF-α when reconstituted with 1.0 mL of reagent diluent. Dilute to a working concentration of 100 ng/mL in reagent diluent.
- **Standard** - 150 ng/mL of recombinant rat TNF-α when reconstituted with 0.5 mL of reagent diluent. Allow the standard to sit for a minimum of 15 minutes with gentle agitation prior to making dilutions. A seven point standard curve using 2-fold serial dilutions in reagent diluent, and a high standard of 4000 pg/mL is recommended.

- **Streptavidin-HRP** - 1.0 mL of streptavidin conjugated to horseradish-peroxidase. Dilute to the working concentration specified on the vial label using reagent diluent.

Plate Preparation

1. Dilute the capture antibody to the working concentration in PBS without carrier protein. Immediately coat a 96-well microplate with 100 µL per well of the diluted capture antibody. Seal the plate and incubate overnight at room temperature.
2. Aspirate each well and wash with wash buffer, repeating the process two times for a total of three washes. Wash by filling each well with wash buffer (400 µL) using a squirt bottle, manifold dispenser or autowasher. Complete removal of liquid at each step is essential for good performance. After the last wash, remove any remaining wash buffer by aspirating or by inverting the plate and blotting it against clean paper towels.
3. Block plates by adding 300 µL of reagent diluent to each well. Incubate at room temperature for a minimum of 1 hour.
4. Repeat the aspiration/wash as in step 2. The plates are now ready for sample addition.

Assay Procedure

1. Add 100 µL of sample or standards in reagent diluent, or an appropriate diluent, per well. Cover with an adhesive strip and incubate 2 hours at room temperature.
2. Repeat the aspiration/wash as in step 2 of Plate Preparation.
3. Add 100 µL of the detection antibody, diluted in reagent diluent, to each well. Cover with a new adhesive strip and incubate 2 hours at room temperature.
4. Repeat the aspiration/wash as in step 2 of Plate Preparation.

5. Add 100 µL of the working dilution of Streptavidin-HRP to each well. Cover the plate and incubate for 20 minutes at room temperature. Avoid placing the plate in direct light.

6. Repeat the aspiration/wash as in step 2.

7. Add 100 µL of substrate solution to each well. Incubate for 20 minutes at room temperature. Avoid placing the plate in direct light.

8. Add 100 µL of stop solution to each well. Gently tap the plate to ensure thorough mixing.

9. Determine the optical density of each well immediately, using a microplate reader set to 450 nm. If wavelength correction is available, set to 540 nm or 570 nm. If wavelength correction is not available, subtract readings at 540 nm or 570 nm from the readings at 450 nm. This subtraction will correct for optical imperfections in the plate.

Readings made directly at 450 nm without correction may be higher and less accurate.

Appendix E. IL-6 ELISA Protocol

(Catalog Number: DY506 (R&D Systems, Inc.)

Materials and solutions required:

- **ELISA High Binding plates** - Greiner Microlon LE High Binding Plates
- **Phosphate Buffered Saline**
- **Wash Buffer** - Biosource 25X Wash Buffer (WB01/Q110408)) – diluted with deionized water to 1X
- **Reagent Diluent** - 1% BSA Calbiochem (Cat#12659) in PBS
- **Substrate Solution** - KPL SureBlue Reserve TMB 1-Component Microwell Peroxidase Substrate (Cat #:53-00-03)
- **Stop Solution** – KPL TMB Stop Solution (Cat#:50-85-05)
- **Stimulant** - Lipopolysaccharide (LPS): Sigma-Aldrich (Cat#:L2630)
- **Capture Antibody** - 720 µg/mL of mouse anti-rat IL-6 when reconstituted with 1.0 mL of PBS. Dilute to a working concentration of 4.0 µg/mL in PBS, without carrier protein.
- **Detection Antibody** - 72 µg/mL of biotinylated goat anti-rat IL-6 when reconstituted with 1.0 mL of reagent diluent. Dilute to a working concentration of 400 ng/mL in reagent diluent.
- **Standard** - 250 ng/mL of recombinant rat IL-6 when reconstituted with 0.5 mL of reagent diluent. Allow the standard to sit for a minimum of 15 minutes with gentle agitation prior to making dilutions. A seven point standard curve using 2-fold serial dilutions in reagent diluent, and a high standard of 8000 pg/mL is recommended.

- **Streptavidin-HRP** - 1.0 mL of streptavidin conjugated to horseradish-peroxidase. Dilute to the working concentration specified on the vial label using reagent diluent.

Plate Preparation

1. Dilute the capture antibody to the working concentration in PBS without carrier protein. Immediately coat a 96-well microplate with 100 µL per well of the diluted capture antibody. Seal the plate and incubate overnight at room temperature.
2. Aspirate each well and wash with wash buffer, repeating the process two times for a total of three washes. Wash by filling each well with wash buffer (400 µL) using a squirt bottle, manifold dispenser or autowasher. Complete removal of liquid at each step is essential for good performance. After the last wash, remove any remaining wash buffer by aspirating or by inverting the plate and blotting it against clean paper towels.
3. Block plates by adding 300 µL of reagent diluent to each well. Incubate at room temperature for a minimum of 1 hour.
4. Repeat the aspiration/wash as in step 2. The plates are now ready for sample addition.

Assay Procedure

1. Add 100 µL of sample or standards in reagent diluent, or an appropriate diluent, per well. Cover with an adhesive strip and incubate 2 hours at room temperature.
2. Repeat the aspiration/wash as in step 2 of Plate Preparation.
3. Add 100 µL of the detection antibody, diluted in reagent diluent, to each well. Cover with a new adhesive strip and incubate 2 hours at room temperature.
4. Repeat the aspiration/wash as in step 2 of Plate Preparation.

5. Add 100 µL of the working dilution of Streptavidin-HRP to each well. Cover the plate and incubate for 20 minutes at room temperature. Avoid placing the plate in direct light.

6. Repeat the aspiration/wash as in step 2.

7. Add 100 µL of substrate solution to each well. Incubate for 20 minutes at room temperature. Avoid placing the plate in direct light.

8. Add 100 µL of stop solution to each well. Gently tap the plate to ensure thorough mixing.

9. Determine the optical density of each well immediately, using a microplate reader set to 450 nm. If wavelength correction is available, set to 540 nm or 570 nm. If wavelength correction is not available, subtract readings at 540 nm or 570 nm from the readings at 450 nm. This subtraction will correct for optical imperfections in the plate.

Readings made directly at 450 nm without correction may be higher and less accurate.

Bibliography

American Conference of Governmental and Industrial Hygienists (ACGIH) Threshold Limit Value (TLV) Guide, 2006.

American Type Culture Collection. http://www.atcc.org/common/catalog/numSearch/numResults.cfm?atccNum=CRL-2192. 13 June 2007.

Athanassiou, E. K., R. N. Grass, and W. J. Stark. "Large-scale production of carbon-coated copper nanoparticles for sensor applications," *Nanotechnology,* 17(6): 1668-1673 (2006).

Barceloux, Donald. G. "Copper," *Clinical toxicology,* 37(2): 217-230 (1999).

Barrabés, N., J. Just, A. Dafinov, F. Medina, J. L. G. Fierro, J. E. Sueiras, P. Salagre, and Y. Cesteros. "Catalytic reduction of nitrate on pt-cu and pd-cu on active carbon using continuous reactor: The effect of copper nanoparticles," *Applied Catalysis B: Environmental,* 62(1-2): 77-85 (January 2006).

Bates, David. V., Birney R. Fish, Theodore F. Hatch, Thomas T. Mercer, and Paul E. Morrow. "Deposition and retention models for internal dosimetry of the human respiratory tract. task group on lung dynamics," *Health physics,* 12(2): 173-207 (1966).

Bermudez, Edilberto, James B. Mangum, Brian A. Wong, Bahman Asgharian, Paul M. Hext, David B. Warheit, and Jeffrey I. Everitt. "Pulmonary responses of mice, rats, and hamsters to subchronic inhalation of ultrafine titanium dioxide particles," *Toxicological Sciences,* 77(2): 347-357 (2004).

Bertinato, Jesse, and Mary R. L'Abbé. "Maintaining copper homeostasis: Regulation of copper-trafficking proteins in response to copper deficiency or overload," *The Journal of Nutritional Biochemistry,* 15(6): 316-322 (June 2004).

Bondeson, Jan. "The mechanisms of action of disease-modifying antirheumatic drugs: A review with emphasis on macrophage signal transduction and the induction of proinflammatory cytokines," *General Pharmacology: The Vascular System,* 29(2): 127-150 (August 1997).

Braydich-Stolle, Laura, Saber Hussain, John J. Schlager, and Marie-Claude Hofmann. "In vitro cytotoxicity of nanoparticles in mammalian germline stem cells," *Toxicological Sciences,* 88(2): 412-419 (2005).

Bremner, Ian. "Manifestations of copper excess," *American Journal of Clinical Nutrition,* 67(5): 1069S-1073S (1998).

Chellat, Fatiha, Yahye Merhi, Alain Moreau, and L'Hocine Yahia. "Therapeutic potential of nanoparticulate systems for macrophage targeting," *Biomaterials,* 26(35): 7260-7275 (December 2005).

Chen, Chun-Chin, and Franklin C. Hong. "Structure and properties of diamond-like carbon nanocomposite films containing copper nanoparticles," *Applied Surface Science,* 242(3-4): 261-269 (April 2005).

Chen, Yuxiang, Zhigang Xue, Duo Zheng, Kun Xia, Yanzhong Zhao, Ting Liu, Zhigao Long, and Jiahui Xia. "Sodium chloride modified silica nanoparticles as a non-viral vector with a high efficiency of DNA transfer into cells," *Current Gene Therapy*, 3: 273-279 (2003).

Chen, Zhen, Huan Meng, Gengmei Xing, Chunying Chen, Yuliang Zhao, Guang Jia, Tiancheng Wang, Hui Yuan, Chang Ye, Feng Zhao, Zhifang Chai, Chuanfeng Zhu, Xiaohong Fang, Baocheng Ma, and Lijun Wan. "Acute toxicological effects of copper nanoparticles in vivo," *Toxicology Letters,* 163(2): 109-120 (May 2006).

Cioffi, N., N. Ditaranto, L. Torsi, R. A. Picca, L. Sabbatini, A. Valentini, L. Novello, G. Tantillo, T. Bleve-Zacheo, and P. G. Zambonin. "Analytical characterization of bioactive fluoropolymer ultra-thin coatings modified by copper nanoparticles," *Analytical and Bioanalytical Chemistry,* 381(3): 607-616 (2005).

Colvin, Vicki L. "The potential environmental impact of engineered nanomaterials," *Nature Biotechnology,* 21(10): 1166-1170 (2003).

Diabaté, Silvia, Sonja Mülhopt, Hanns-R Paur, Ralf Wottrich, and Harald F. Krug. "In vitro effects of incinerator fly ash on pulmonary macrophages and epithelial cells," *International Journal of Hygiene and Environmental Health,* 204(5-6): 323-326 (2002).

Defense Nanotechnology Research and Development Program, 26 April 2007.

Dietary Reference Intakes for Vitamin A, Vitamin K, Arsenic, Boron, Chromium, Copper, Iodine, Iron, Manganese, Molybdenum, Nickel, Silicon, Vanadium and Zinc. Washington, DC: National Academies Press, July 2002.

DoD Funds Model Development to Predict Nanoparticle Effects on Living Systems. http://www.nano.gov/html/news/Oberdorster_Article.htm. 29 March 07

Donaldson, K., X. Y. Li, and W. MacNee. "Ultrafine (nanometre) particle mediated lung injury," *Journal of Aerosol Science,* 29(5-6): 553-560 (June 1998).

Dörger, Martina, Silvia Münzing, Anne-Marie Allmeling, Konrad Messmer, and Fritz Krombach. "Differential responses of rat alveolar and peritoneal macrophages to man-made vitreous fibers in vitro," *Environmental Research,* 85(3): 207-214 (March 2001).

Dörger, Martina, Anne-Marie Allmeling, Ariane Neuber, Jurgen Behr, Walter Rambeck, and Fritz Krombach. "Interspecies comparison of rat and hamster alveolar macrophage antioxidative and oxidative capacity," *Environmental health perspectives,* 105(Supplement 5): 1309-1312 (1997).

Dörger, Martina, Silvia Münzing, Anne-Marie Allmeling, Konrad Messmer, and Silvia F. Krombach. "Phenotypic and functional differences between rat alveolar, pleural, and peritoneal macrophages," *Experimental Lung Research*, 27: 65-76 (2001).

Dörger, Martina, and Fritz Krombach. "Response of alveolar macrophages to inhaled particulates," *European Surgical Research,* 34(1): 47-52 (2002).

Dorsey, Alfred, Lisa Ingerman, and Steven Swarts, "Toxicological Profile for Copper," United States Department of Health and Human Services, Public Health Service, Agency for Toxic Substances and Disease Registry (ATSDR) (September 2004).

Dowling, Ann P. "Development of nanotechnologies," *Materials Today,* 7(Supplement 1): 30-35 (December 2004).

Driscoll, Kevin E., Janet M. Carter, Diana G. Hassenbein, and Brian Howard. "Cytokines and particle-induced inflammatory cell recruitment," *Environmental health perspectives,* 105(Supplement 5): 1159-1164 (1997).

Dumortier, Helene, Stephanie Lacotte, Giorgia Pastorin, Riccardo Marega, Wei Wu, Davide Bonifazi, Jean-Paul Briand, Maurizo Prato, Sylviane Muller, and Alberto Bianco. "Functionalized carbon nanotubes are non-cytotoxic and preserve the functionality of primary immune cells," *Nano Letters,* 6(7): 1522-1528 (2006).

Feliciani, C., A. K. Gupta, and D. N. Sauder. "Keratinocytes and cytokine/growth factors," *Critical Reviews in Oral Biology Medicine,* 7(4): 300-318 (1996).

Foley, Sarah, Colin Crowley, Monique Smaihi, Claude Bonfils, Bernard F. Erlanger, Patrick Seta, and Christian Larroque. "Cellular localisation of a water-soluble fullerene derivative," *Biochemical and Biophysical Research Communications,* 294(1): 116-119 (May 2002).

Forman, Henry J., and Martine Torres. "Redox signaling in macrophages," *Molecular Aspects of Medicine,* 22(4-5): 189-216 (2001).

Freedman, Jonathan H., Maria R. Ciriolo, and Jack Peisach. 'The role of glutathione in copper metabolism and toxicity," *Journal of Biological Chemistry,* 264(10): 5598-5605 (1989).

Gaetke, Lisa M., and Ching K. Chow. "Copper toxicity, oxidative stress, and antioxidant nutrients," *Toxicology,* 189(1-2): 147-163 (July 2003).

Gardner, Donald. E. "Alterations in macrophage functions by environmental chemicals," *Environmental health perspectives,* 55: 343-358 (1984).

Griffitt, Robert J., Roxana Weil, Kelly A. Hyndman, Nancy D. Denslow, Kevin Powers, David Taylor, and David S. Barber. "Exposure to copper nanoparticles causes gill injury and acute lethality in zebrafish (danio rerio)," *Environmental Science & Technology,* 41(23): 8178-8186 (2007).

Halliwell, Barry and John M. C. Gutteridge. "Oxygen toxicity, oxygen radicals, transition metals and disease," *Biochem Journal*, 219: 1-14 (1984).

Hoet, Peter H., Irene Bruske-Hohlfeld, and Oleg V. Salata. "Nanoparticles - known and unknown health risks," *Journal of nanobiotechnology,* 2(1): 12 (2004).

Holsapple, Michael P., William H. Farland, Timothy D. Landry, Nancy A. Monteiro-Riviere, Janet M. Carter, Nigel J. Walker, and Karluss V. Thomas. "Research strategies for safety evaluation of nanomaterials, part II: Toxicological and safety evaluation of nanomaterials, current challenges and data needs," *Toxicological Sciences,* 88(1): 12-17 (2005).

House, Robert V. "Theory and practice of cytokine assessment in immunotoxicology," *Methods,* 19(1): 17-27 (1999).

House, Robert V. "Cytokine measurement techniques for assessing hypersensitivity," *Toxicology,* 158(1-2): 51-58 (2001).

Hussain, S. M., K. L. Hess, J. M. Gearhart, K. T. Geiss, and J. J. Schlager. "In vitro toxicity of nanoparticles in BRL 3A rat liver cells," *Toxicology in Vitro,* 19(7): 975-983 (October 2005).

Hussain, Saber M., and John M. Frazier. "Cellular toxicity of hydrazine in primary rat hepatocytes," *Toxicological Sciences,* 69(2): 424-432 (2002).

Jesch, Natalite K., Martina Dorger, Georg Enders, Gabriele Rieder, Claus Vogelmeier, Konrad Messmer, and Fritz Krombach. "Expression of inducible nitric oxide synthase and formation of nitric oxide by alveolar macrophages: An interspecies comparison," *Environmental health perspectives,* 105(Supplement) 5: 1297-1300 (1997).

Jonsson, Charlotte A. and Hans Carlsten. "Mycophenolic acid inhibits inosine 5'-monophosphate dehydrogenase and suppresses immunoglobulin and cytokine production of B cells," *International immunopharmacology,* 3(1): 31-37 (2003).

Kim, Jun S., Tae-Jong Yoon, Kyeong N. Yu, Byung G. Kim, Sung J. Park, Hyun W. Kim, Kee H. Lee, Seung B. Park, Jin-Kyu Lee, and Myung H. Cho. "Toxicity and tissue distribution of magnetic nanoparticles in mice," *Toxicological Sciences,* 89(1): 338-347 (2006).

Kreuter, Jörg. "Nanoparticulate systems for brain delivery of drugs," *Advanced Drug Delivery Reviews,* 47(1): 65-81 (March 2001).

Krombach, Fritz, Silvia Munzing, Anne-Marie Allmeling, J. Tilman Gerlach, Jurgen Behr, and Martina Dorger. "Cell size of alveolar macrophages: An interspecies comparison," *Environmental health perspectives,* 105(Supplement 5): 1261-1263 (1997).

Lam, Chiu-Wing, John T. James, Richard McCluskey, and Robert L. Hunter. "Pulmonary toxicity of single-wall carbon nanotubes in mice 7 and 90 days after intratracheal instillation," *Toxicological Sciences,* 77(1): 126-134 (2004).

Laskin, Debra L., and Jeffrey D. Laskin. "Role of macrophages and inflammatory mediators in chemically induced toxicity," *Toxicology,* 160(1-3): 111-118 (2001).

Lehnert, Bruce E. "Pulmonary and thoracic macrophage subpopulations and clearance of particles from the lung," *Environmental health perspectives,* 97: 17-46 (1992).

Lemaire, Irma, and Sophie Ouellet. "Distinctive profile of alveolar macrophage-derived cytokine release induced by fibrogenic and nonfibrogenic mineral dusts," *Journal of toxicology and environmental health,* 47(5): 465-478 (1996).

Li, C-M., H. Lei, Y-J. Tang, J-S. Luo, W. Liu, and Z-M. Chen. "Production of copper nanoparticles by the flow-levitation method," *Nanotechnology,* 15(12): 1866-1869 (2004).

Li, Ying-Hua, Anneue Brauner, Baldvin Jonsson, Ingeborg van der Ploeg, Olle Soder, Mikael Holst, Jorgen Skov Jensen, Hugo Lagercrantz, and Kjell Tullus. "Ureaplasma urealyticum-induced production of proinflammatory cytokines by macrophages," *Pediatric research,* 48(1): 114-119 (2000).

Linder, Maria C., and Maryam Hazegh-Azam. "Copper biochemistry and molecular biology," *American Journal of Clinical Nutrition,* 63(5): 797S-811S (1996).

Liu, G., X. Li, B. Qin, D. Xing, Y. Guo, and R. Fan. "Investigation of the mending effect and mechanism of copper nano-particles on a tribologically stressed surface," *Tribology letters,* 17(4): (2004).

Liu, Yueqiang, Sara A. Majetich, Robert D. Tilton, David S. Sholl, and Gregory V. Lowry. "TCE dechlorination rates, pathways, and efficiency of nanoscale iron particles with different properties," *Environmental Science & Technology,* 39(5): 1338-1345 (2005).

Losa Garcia, J. E., F. M. Rodriguez, M. R. Martin de Cabo, M. J. Garcia Salgado, J. P. Losada, L. G. Villaron, A. J. Lopez, and J. L. Arellano. "Evaluation of inflammatory cytokine secretion by human alveolar macrophages," *Mediators of inflammation,* 8(1): 43-51 (1999).

Lyon, Delina Y., Laura K. Adams, Joshua C. Falkner, and Pedro J. J. Alvarez. "Antibacterial activity of fullerene water suspensions: Effects of preparation method and particle size," *Environmental Science & Technology,* 40(14): 4360-4366 (2006).

Major, Jennifer, Julia E. Fletcher, and Thomas A. Hamilton. "IL-4 pretreatment selectively enhances cytokine and chemokine production in lipopolysaccharide-stimulated mouse peritoneal macrophages," *The Journal of Immunology,* 168(5): 2456-2463 (2002).

Martin, Linda D., Thomas M. Krunkosky, Janice A. Dye, Bernard M. Fischer, Nan Fei Jiang, Lori G. Rochelle, Nancy J. Akley, Kevin L. Dreher, and Kenneth B. Adler. "The role of reactive oxygen and nitrogen species in the response of airway epithelium to particulates," *Environmental health perspectives,* 105(Supplement 5): 1301-1307 (1997).

Maynard, Andrew D., Paul A. Baron, Michael Foley, Anna A. Shvedova, Elena R. Kisin, and Vincent Castranova. "Exposure to carbon nanotube material: Aerosol release during the handling of unrefined single-walled carbon nanotube material," *Journal of toxicology and environmental health, Part A,* 67(1): 87-107 (2004).

McRitchie, DonnaI, Noritaka Isowa, JeffreyD Edelson, Alexandre M. Xavier, Lu Cai, Heng-Ye Man, YuTian Wang, ShafH Keshavjee, Arthur S. Slutsky, and Mingyao Liu. "Production of tumour necrosis Factor α by primary cultured rat alveolar epithelial cells," *Cytokine,* 12(6): 644-654 (2000).

Meng, Huan, Zhen Chen, Gengmei Xing, Hui Yuan, Chunying Chen, Feng Zhao, Chengcheng Zhang, Yun Wang, and Yuliang Zhao. "Ultrahigh reactivity and grave nanotoxicity of copper nanoparticles," *Journal of Radioanalytical and Nuclear Chemistry,* 272(3): 595-598 (2007).

Moore, M. N. "Do nanoparticles present ecotoxicological risks for the health of the aquatic environment?," *Environment International,* 32(8): 967-976 (December 2006).

Morgan, Daniel L., and Cassandra J. Shines. "Alveolar macrophage cytotoxicity for normal lung fibroblasts is mediated by nitric oxide release," *Toxicology in Vitro,* 18(1): 139-146 (February 2004).

Morrison, M. L., R. A. Buchanan, P. K. Liaw, C. J. Berry, R. L. Brigmon, L. Riester, H. Abernathy, C. Jin, and R. J. Narayan. "Electrochemical and antimicrobial properties of diamondlike carbon-metal composite films," *Diamond and Related Materials,* 15(1): 138-146 (January 2006).

Mukhopadhyay, Srirupa, John R. Hoidal, and Tapan K. Mukherjee. "Role of TNFalpha in pulmonary pathophysiology," *Respiratory research,* 7125 (2006).

National Nanotechnology Initiative. http://clinton4.nara.gov/WH/New/html/20000121_4.html. 18 June 2007.

Oberdorster, E. "Manufactured nanomaterials (fullerenes, C60) induce oxidative stress in the brain of juvenile largemouth bass," *Environmental health perspectives,* 112(10): 1058-1062 (2004).

Oberdorster, Gunter., Juraj Ferin, Robert Gelein, Sidney C. Soderholm, and Jacob Finkelstein. "Role of the alveolar macrophage in lung injury: Studies with ultrafine particles," *Environmental health perspectives,* 97: 193-199 (1992).

Oberdorster, Gunter, Juraj Ferin, and Bruce E. Lehnert. "Correlation between particle size, in vivo particle persistence, and lung injury," *Environmental health perspectives,* 102(Supplement 5): 173-179 (1994).

Oberdorster, Gunter, Eva Oberdorster, and Jan Oberdorster. "Nanotoxicology: An emerging discipline evolving from studies of ultrafine particles," Environmental health perspectives, 113(7): 823-839 (July 2005).

Paine III, Robert, Susan B. Morris, Hong Jin, Steven E. Wilcoxen, Susan M. Phare, Bethany B. Moore, Michael J. Coffey, and Galen B. Toews. "Impaired functional activity of alveolar macrophages from GM-CSF-deficient mice," *AJP - Lung Cellular and Molecular Physiology,* 281(5): L1210-L1218 (2001).

Panyam, Jayanth, and Vinod Labhasetwar. "Biodegradable nanoparticles for drug and gene delivery to cells and tissue," *Advanced Drug Delivery Reviews,* 55(3): 329-347 (February 2003).

Ponce, Aldo A., and Kenneth J. Klabunde. "Chemical and catalytic activity of copper nanoparticles prepared via metal vapor synthesis," *Journal of Molecular Catalysis A: Chemical,* 225(1): 1-6 (January 2005).

Promega CellTiter 96® AQ_{ueous} One Solution Cell Proliferation Assay Technical Bulletin (April 2005).

Promega CytoTox-ONE™ Homogenous Membrane Integrity Assay Technical Bulletin (January 2006).

R&D Systems, Inc., rat IL-6 DuoSet ELISA Development Kit (Catalog Number:DY506) (February 2007).

R&D Systems, Inc., rat TNF-α/TNFSF1A DuoSet ELISA Development Kit (Catalog Number:DY510) (January 2006).

Renwick, L. C., K. Donaldson, and A. Clouter. "Impairment of alveolar macrophage phagocytosis by ultrafine particles," *Toxicology and Applied Pharmacology,* 172(2): 119-127 (April 2001).

Rice, Timothy M., Robert W. Clarke, John J. Godleski, Eiman Al-Mutairi, Nan-Fei Jiang, Russ Hauser, and Joseph D. Paulauskis. "Differential ability of transition metals to induce pulmonary inflammation," *Toxicology and Applied Pharmacology,* 177(1): 46-53 (November 2001).

Rorabacher, D. B. "Statistical treatment for rejection of deviant values: Critical values of dixon's "Q" parameter and related subrange ratios at the 95% confidence level," *Analytical Chemistry (Washington),* 63(2): 139 (1991).

Rubin, Bernard, Gary S. Firestein, and Leonard H. Calabrese. "The Role of IL-6 in Inflammatory Diseases," www.medscape.com. 8 November 2007.

Schmalz, G., U. Schuster, and H. Schweikl. "Influence of metals on IL-6 release in vitro," *Biomaterials,* 19(18): 1689-1694 (1998).

Schrick, Bettina, Bianca W. Hydutsky, Jennifer L. Blough, and Thomas E. Mallouk. "Delivery vehicles for zerovalent metal nanoparticles in soil and groundwater," *Chemistry of Materials,* 16(11): 2187-2193 (2004).

Seth, R., S. Yang, S. Choi, M. Sabean, and E. A. Roberts. "In vitro assessment of copper-induced toxicity in the human hepatoma line, hep G2," *Toxicology in Vitro,* 18(4): 501-509 (August 2004).

Sies, H. "Oxidative stress: Oxidants and antioxidants," *Experimental Physiology,* 82(2): 291-295 (1997).

Sies, Helmut. "Glutathione and its role in cellular functions," *Free Radical Biology and Medicine,* 27(9-10): 916-921 (November 1999).

Stohs, S. J., and D. Bagchi. "Oxidative mechanisms in the toxicity of metal ions," *Free Radical Biology and Medicine,* 18(2): 321-336 (February 1995).

Suska, F., M. Esposito, C. Gretzer, M. Källtorp, P. Tengvall, and P. Thomsen. "IL-1α, IL-1β and TNF-α secretion during in vivo/ex vivo cellular interactions with titanium and copper," *Biomaterials,* 24(3): 461-468 (2003).

Tan, Shirlee, Yutaka Sagara, Yuanbin Liu, Pamela Maher, and David Schubert. "The regulation of reactive oxygen species production during programmed cell death," *The Journal of Cell Biology,* 141(6): 1423-1432 (1998).

Tarasov, S., A. Kolubaev, S. Belyaev, M. Lerner, and F. Tepper. "Study of friction reduction by nanocopper additives to motor oil," *Wear,* 252(1-2): 63-69 (January 2002).

Teeguarden, Justin G., Paul M. Hinderliter, Galya Orr, Brian D. Thrall, and Joel G. Pounds. "Particokinetics in vitro: Dosimetry considerations for in vitro nanoparticle toxicity assessments," *Toxicological Sciences,* 95(2): 300-312 (2007).

Thomas, Karluss, and Philip Sayre. "Research strategies for safety evaluation of nanomaterials, part I: Evaluating the human health implications of exposure to nanoscale materials," *Toxicological Sciences,* 87(2): 316-321 (2005).

Trohalaki, Steven, Robert J. Zellmer, Ruth Pachter, Saber M. Hussain, and John M. Frazier. "Risk assessment of high-energy chemicals by in vitro toxicity screening and quantitative structure-activity relationships," *Toxicological Sciences,* 68(2): 498-507 (2002).

Tsuji, Joyce S., Andrew D. Maynard, Paul C. Howard, John T. James, Chiu-wing Lam, David B. Warheit, and Annette B. Santamaria. "Research strategies for safety evaluation of nanomaterials, part IV: Risk assessment of nanoparticles," *Toxicological Sciences,* 89(1): 42-50 (2006).

United States Environmental Protection Agency Copper Drinking Water. http://www.epa.gov/safewater/contaminants/index.html. 9 July 07

United States Environmental Protection Agency Nanotechnology. http://es.epa.gov/ncer/nano/questions/index.html. 21 June 2007.

Vauthier, Christine, Catherine Dubernet, Elias Fattal, Huguette Pinto-Alphandary, and Patrick Couvreur. "Poly(alkylcyanoacrylates) as biodegradable materials for biomedical applications," *Advanced Drug Delivery Reviews,* 55(4): 519-548 (2003).

Wagner, Andrew J., Charles A. Bleckmann, Richard C. Murdock, Amanda M. Schrand, John J. Schlager, and Saber M. Hussain. "Cellular interaction of different forms of aluminum nanoparticles in rat alveolar macrophages," *Journal of Physical Chemistry B,* 111(25): 7353-7359 (2007).

Wang, Hong, and James A. Joseph. "Quantifying cellular oxidative stress by dichlorofluorescein assay using microplate reader," *Free Radical Biology and Medicine,* 27(5-6): 612-616 (September 1999).

Warheit, D. B., J. F. Hansen, I. S. Yuen, D. P. Kelly, S. I. Snajdr, and M. A. Hartsky. "Inhalation of high concentrations of low toxicity dusts in rats results in impaired pulmonary clearance mechanisms and persistent inflammation," *Toxicology and Applied Pharmacology,* 145(1): 10-22 (July 1997).

Warheit, D. B., B. R. Laurence, K. L. Reed, D. H. Roach, G. A. M. Reynolds, and T. R. Webb. "Comparative pulmonary toxicity assessment of single-wall carbon nanotubes in rats," *Toxicological Sciences,* 77(1): 117-125 (2004).

Waris, Gulam, and Haseeb Ahsan. "Reactive oxygen species: Role in the development of cancer and various chronic conditions," *Journal of Carcinogenesis,* 514 (2006).

Wataha, John C., Carl T. Hanks, and Zhilin Sun. "In vitro reaction of macrophages to metal ions from dental biomaterials," *Dental Materials,* 11(4): 239-245 (1995).

Wilson, Martin R., Laurent Foucaud, Peter G. Barlow, Gary R. Hutchison, Jill Sales, Richard J. Simpson, and Vicki Stone. "Nanoparticle interactions with zinc and iron: Implications for toxicology and inflammation," *Toxicology and applied pharmacology,* 225(1): 80-89 (2007).

Xu, Cailu, Gongwei Wu, Zheng Liu, Dehai Wu, Thomas T. Meek, and Qingyou Han. "Preparation of copper nanoparticles on carbon nanotubes by electroless plating method," *Materials Research Bulletin,* 39(10): 1499-1505 (August 2004).

Yoon, Ki-Young, Jeong Hoon Byeon, Jae-Hong Park, and Jungho Hwang. "Susceptibility constants of escherichia coli and bacillus subtilis to silver and copper nanoparticles," *Science of The Total Environment,* 373(2-3): 572-575 (February 2007).

Zhang, X. F., X. L. Dong, H. Huang, D. K. Wang, B. Lv, and J. P. Lei. "High permittivity from defective carbon-coated cu nanocapsules," *Nanotechnology,* 18(27) (2007).

Vita

Capt Brian Clarke was born and raised in Tacoma, WA. He entered the United States Air Force Academy in 1999. Upon graduation in 2003 with a Bachelors of Science degree in Biology, Capt Clarke earned a commission into the Biomedical Science Corp and the Bioenvironmental Engineering career field. He completed the initial Bioenvironmental Engineering Officer's course at Brooks City-Base, TX in November 2003 as an honor graduate. Capt Clarke's first assignment was at Moody Air Force Base, GA, where he served as the Chief, Industrial Hygiene Programs and Deputy Flight Commander of the Bioenvironmental Engineering Flight.

In August 2006, Capt Clarke entered the Air Force Institute of Technology Environmental Engineering and Science degree program. After completion of his degree, he will be assigned to the Air Force Institute of Operational Health's Environmental Analysis Section at Brooks City-Base.

e public reporting burden for this collection of information is estimated to average 1 hour per response, including the time for reviewing instructions, searching existing data sources, gathering and maintaining the data needed, and completing and reviewing the collection of information. Send comments regarding this burden estimate or any other aspect of the collection of information, including suggestions for reducing this burden to Department of Defense, Washington Headquarters Services, Directorate for Information Operations and Reports (0704-0188), 1215 Jefferson Davis Highway, Suite 1204, Arlington, VA 22202-4302. Respondents should be aware that notwithstanding any other provision of law, no person shall be subject to an penalty for failing to comply with a collection of information if it does not display a currently valid OMB control number.
PLEASE DO NOT RETURN YOUR FORM TO THE ABOVE ADDRESS.

1. REPORT DATE *(DD-MM-YYYY)*	2. REPORT TYPE	3. DATES COVERED *(From – To)*
27-03-2008	**Master's Thesis**	March 2007 – March 2008

4. TITLE AND SUBTITLE

***In vitro* Toxicity and Inflammation Response Induced by Copper Nanoparticles in Rat Alveolar Macrophages**

5a. CONTRACT NUMBER

5b. GRANT NUMBER

5c. PROGRAM ELEMENT NUMBER

6. AUTHOR(S)

Clarke, Brian, M., Captain, USAF, BSC

5d. PROJECT NUMBER

5e. TASK NUMBER

5f. WORK UNIT NUMBER

7. PERFORMING ORGANIZATION NAMES(S) AND ADDRESS(S)

Air Force Institute of Technology
Graduate School of Engineering and Management (AFIT/EN)
2950 Hobson Way
WPAFB OH 45433-7765

8. PERFORMING ORGANIZATION REPORT NUMBER

AFIT/GES/ENV/08-M01

9. SPONSORING/MONITORING AGENCY NAME(S) AND ADDRESS(ES)

Hussain, Saber M. Civ AFRL/RHPB
Air Force Research Lab (AFMC)
Bldg 837, Area B, 2729 R Street
WPAFB, OH 45433-7765
Tel: 937-904-9517 (email: saber.hussain@wpafb.af.mil)

10. SPONSOR/MONITOR'S ACRONYM(S)

11. SPONSOR/MONITOR'S REPORT NUMBER(S)

12. DISTRIBUTION/AVAILABILITY STATEMENT

APPROVED FOR PUBLIC RELEASE; DISTRIBUTION UNLIMITED.

13. SUPPLEMENTARY NOTES

14. ABSTRACT

Nanotechnology is a thriving industry and has the potential to benefit society in numerous ways. However, not all environmental and human health concerns of nanomaterials have been addressed. Thus, the purpose of this research was to investigate the toxicity and inflammation potential (using cytokines TNF-α and IL-6 as indicators) of various sized copper nanoparticles (40, 60, and 80 nm) in rat alveolar macrophages. Toxicity measurements were accomplished by means of *in vitro* techniques and toxicity mechanisms were studied by measuring reactive oxygen species (ROS) production. In addition, cytokine measurements used enzyme-linked immunosorbent assay (ELISA) methods. Results show copper nanoparticles as gravely toxic to rat alveolar macrophages; concentrations of only 10 µg/mL produced cell viability of less than 20 percent and membrane leakage increases of approximately 75 percent. However, the copper nanoparticles did not produce a significant degree of ROS (only 2.5 fold increases). Also, the toxicity showed a dose-dependent relationship, but not a significant size dependency between the various sized copper nanoparticles. Finally, minimal induction of cytokines occurred; however, stimulation of rat alveolar macrophages by lipopolysaccharide (LPS) and subsequent exposure to copper nanoparticles produced elevated levels of both cytokines.

15. SUBJECT TERMS

Nanotechnology, Copper Nanoparticles, Alveolar Macrophages, Toxicity, Cytokines

16. SECURITY CLASSIFICATION OF:			17. LIMITATION OF ABSTRACT	18. NUMBER OF PAGES	19a. NAME OF RESPONSIBLE PERSON
a. REPORT	b. ABSTRACT	c. THIS PAGE			Bleckmann, Charles A.
U	U	U	UU	100	19b. TELEPHONE NUMBER *(Include area code)* (937) 255-3636, ext 4721 (email: charles.bleckmann@afit.edu)

Standard Form 298 (Rev. 8-98)
Prescribed by ANSI Std. Z39-18